ARCADA

Degree thesis

Deflection study on beams with COMSOL Finite Element Analysis.

Author: Gao Jie

Instructor: Mathew Vihtonen

Degree programme: Materials Processing Technology

20/04/2020

DEGREE THESIS	
Arcada	
Degree Programme:	Materials Processing Technology
Identification number:	19979
Author:	Gao Jie
Title:	Deflection study on beams with COMSOL Finite Element Analysis.
Supervisor (Arcada):	Mathew Vihtonen
Commissioned by:	Silas Gebrehiwot

Abstract:
The main orientation of the thesis is to present and compare the discrepancy between two delegative beam theories which are prevalently applied in both civil engineering and structural analysis. The objectives of the thesis are eventually achieved via Comsol computation and by observing the stress distribution along the beam elements and deformation after importing either a force or moment to the domain. Beams with various thickness and different transverse sections such as square, rectangular and I-beam are input for differentiation.

There are 24 simulation occasions presented in total. By using beam modulus for analysis, to a large degree, results are acquired more accurate when compared with the mathematical calculations on both critical values of stress and displacement than ones from solid mechanics. In conclusion, when objects of a still length are under study for both bending and torsion cases, if the thickness of beams increases, Timoshenko Theory can result more precise on deformation (larger displacement at free end) than Euler-Bernoulli Theory. For instance, the maximum normal stress of square beam due to surface load is 10,5 MPa with displacement of 0,399 mm whereas, both Euler-Bernoulli and Timoshenko formulation manage to obtain the stress value of 10,5 MPa. However, beams under Timoshenko Theory captures a larger displacement with value of 0,345 mm rather than 0,339 mm.

Another parameter which may affect the final findings is the length of the beam. Referring to the concept mentioned in literature review, length-to-thickness ratio somehow will influence precision of results. Hereby, how precise the results are will depend on the length-to-thickness ratio rather than only relying on thickness of the beam.

Keywords:	Euler-Bernoulli Beam Theory, Timoshenko Beam Theory, Finite Element Analysis, Comsol Multiphysics, solid mechanics, beam modulus, bending moment, axial load, torsion.
Number of pages:	85
Language:	English
Date of acceptance:	

ABBREVIATIONS:

T   Traction

ΔS   Small sectional area

ΔF   Distributed forces

σ Stress quantity

σ_{normal} Normal stress

$\vec{n}$ Unit vector

ϑ Included angle

$\vec{v_x}$ Componential vector in x-direction

$\vec{v_y}$ Componential vector in y-direction

$\vec{v_z}$ Componential vector in z-direction

τ shear stress

T_x, T_y, T_z Stress vectors

$\vec{T}$ Total stress vector

E   Elastic modulus of the material

I   Moment of inertia of the cross-sectional area about neutral axis

w(x)   Deflection of the beam in the vertical direction

q   A distributed load

G   Shear modulus of the material

$M_{bending}(x)$ Bending moment

F   Surface load

c   Perpendicular distance from the neutral axis to a point farthest away from the neutral axis.

t   Displacement of between point A and B on the beam

P   Axial loads

ϵ Strain of the beam due to the axial loads

L   Length of the beam

T   Torsion

Ø   angle of twist

A_{square} Cross section area of a square beam

$A_{rectangular}$ Cross section area of a rectangular beam

A_{I-beam} Cross section area of a I beam

 b   width of the cross section

 h   height of the cross section

V   shear force

Contents

PREFACE

I would like to give my sincere appreciations to Mr. Mathew Vihtonen and Mr. Silas Gebrehiwot for their prominent supervision and patient helps throughout my thesis work. Particularly, their professional explanation on relevant theories as well as technical instructions on computational manipulation by which I managed to solve the insurmountable issues encountered during my progress.

Moreover, I have an impressive memory of my four-year experience studying at Arcada University of applied science. I would also like to thank all staff and my teachers for their passion and earnest spirit left to me while I was studying at Arcada. I am truly grateful for the teaching and support from Mathew Vihtonen and Rene Herrmann since they encouraged and enlightened me on the way to my prospective career.

At last, I want to bring my appreciation to my family and my friends for their great support, not only on financial level but also on the mental, throughout four years when I was in Finland. I will hold this power and continue on my further education.

Figures

1. INTRODUCTION

1.1.1. Background

In engineering (exclusively in civil engineering), deflection analysis upon beams, which currently are exerted as the staple materials collaborated with concrete in construction industry, has been being recognised as a significantly indispensable process with the purpose of identifying the critical mechanical deformation magnitude to the beams under various realistic structures. The threshold of analysis is to figure out sorts of deflection which are typically occurred to beams made of different materials. The experimental method is to utilize COMSOL simulator to simulate the deflection that beams inflict when a stress is applied on. Generally, two delegative sorts of beam deflection commonly discussed are put in contrast which indicated visual disparities on angles at the end of ingredients, called Euler-Bernoulli beams and Timoshenko beams, respectively. The conclusions which is presented as well as data collection would be assessed by companies and engineers to predict the quality of texture in bridge constructions and so forth.

1.1.2. Objectives

The research is conducted to investigate the deflection cases on beams with thickness in variety when stress applied. In this study, the objectives are comprised of following steps:

- Studying two main theories of beam's deflection, called Euler-Bernoulli and Timoshenko theory respectively, comprehending all relevant concepts.
- Comparing the disparities between these two theories, collecting properties data of ingredients (elasticity and rigidity etc.) doing data calculation on samples chosen, giving out the hypothesis on the simulation results.

- Simulating the stress behaviour upon beams samples with COMSOL and compare the numbers obtained.
- Analysing the observations and offer the conclusion.

1.1.3. Relevance to working life

According to the conclusions which are determined within the research, realistic fields which are relevant to beam theory integrated on civil engineering, which is the construction of mansions, bridges, tunnels and so forth. Simultaneously, the identical theorem can also be the inspiration to relevance of materials selections.

In addition, for beams with relatively low transverse shear stiffness, the Euler-Bernoulli beam modelling underestimate the deflection. Moreover, the principle of bending vibration is determined based on Euler-Bernoulli theory (Adhikari 2016). By comparison, Timoshenko Beam Theory behaves in transverse shear strain as the length-to-thickness ratio becomes large (Wang & Lee 2000)

To enhance the understanding of two beam theories, some realistic examples are demonstrated as:
Euler-Bernoulli Beam Theory: **Three-point bending, cantilever beam**
Timoshenko Beam Theory: **Thick beam under bending**

2. LITERATURE REVIEW & THEORY DESCRIPTION

2.1. Stress & Strain

Stress and strain are two physical quantities which represent different mechanical behaviour along a selected surface, either internal or external, of a body. Stress is associated with the strength of materials from which the body is made, while strain is a method of measurement which determine the deformation of the body (Hibbeler 2018). Moreover, when investigations of mechanical performance are integrated on properties, materials are supposed to be considered as being continuous, consisting of a continuum or uniform distribution of matter possessing no voids. Materials must be cohesive, parts of which are connected firmly together (Hibbeler 2018 p.40).

2.1.1. Stress

The definition of stress is described as a property which expresses a distribution of force which loads on internal or external surface of the frame. Assuming a concrete body stands beneath a system of forces, whereas the stress field is the distribution of the internal "tractions" T which help balance the external "tractions" and body faces. A concrete body can be subjected to both surface forces and distributed loadings. Surface loads act on a small area of contact are reported by concentrated forces, while distributed loadings are acting over a large surface area of the body.

To exhibit how stress preforms on surfaces, considering that a sectioned area of a substance to be subdivided into several small area ΔS (shown in *Figure 1*). Subsequently, a distribution of loads ΔF is applied at an arbitrary point P when the internal and external forces are acting at the chosen point in opposite directions till the whole system reaches to an equilibrium (Hibbeler 2018).

16
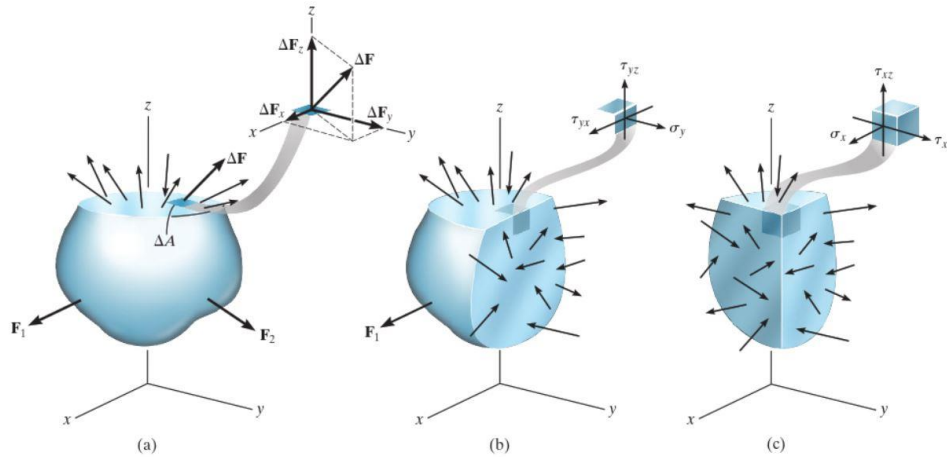
Figure 1. Internal and external forces acting on a body (Hibbeler 2018 p.40)

The traction T is a bound vector which means it cannot slide to another spot with the same definition. Therefore, in a particular direction, the traction can be defined as below.

$$\sigma = \lim_{\Delta s \to 0} \frac{\Delta F}{\Delta S} = \frac{dF}{dS} \tag{2-1}$$

To demonstrate how the internal and external forces are distributed across the intercepted surface at the arbitrary point, a coordinate system is established to reveal the direction of a force applied in the form of vectors $\vec{n}$ (x, y, z). According to directions in discrepancy, the stress which is applied on the intercepted surfaces can be categorized into two types.

1) **normal stress**

Whereas the force is applied perpendicular to the chosen area ΔS. According to the diagram **Figure 2**, to demonstrate the external and internal force distributing across the exposed surface at the arbitrary point, the Cartesian Coordinate is used which indicates components of a force in three-dimension. Hence, normal stress can be described in general as:

$$\sigma_{normal} = \lim_{\Delta S \to 0} \frac{\Delta F}{\Delta S} = \frac{dF_z}{dS} \tag{2-2}$$
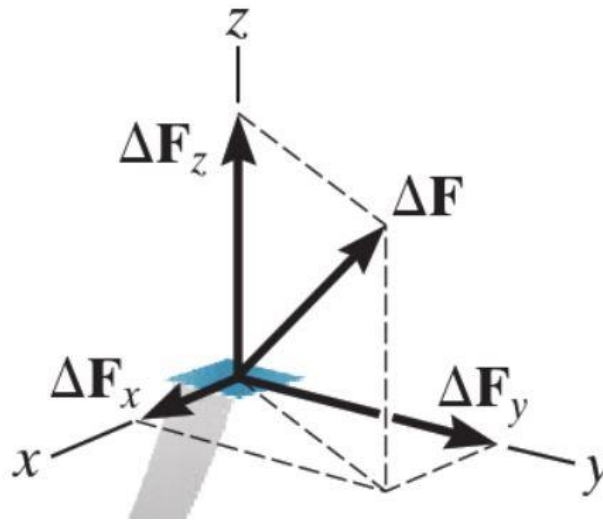
Figure 2. Components of a force along dimensional coordinate. (Hibbleler 2018 p.40)

The vector $\vec{n}$ is the semi-normal of the surface and acts as a unit vector ($x^2 + y^2 + z^2 = 1$). Consisting of three components as the cosines of the angles ϑ between the vector and the coordinate axis (Silva 2006 p.10):

$$\begin{cases} \overrightarrow{v_x} = \cos(v, x) = x \\ \overrightarrow{v_y} = \cos(v, y) = y \\ \overrightarrow{v_z} = \cos(v, z) = z \end{cases} \tag{2-3}$$

Therefore, the normal stress is determined as $\sigma_{normal} = \sigma cos\vartheta = \frac{dF cos\vartheta}{dS}$, perpendicular to the area. According to the convention, stresses which are perpendicular to three different axes are inscribed as σ_x, σ_y and σ_z respectively.

2) shear stress (τ)

The intensity of force acting tangent to the selected area, which is extending along two directions (presented in **Figure 3**) (Hibbeler 2018).

$$\tau_{zx} = \lim_{\Delta S \to 0} \frac{\Delta F_x}{\Delta S} \tag{2-4}$$

$$\tau_{zy} = \lim_{\Delta S \to 0} \frac{\Delta F_y}{\Delta S} \tag{2-5}$$
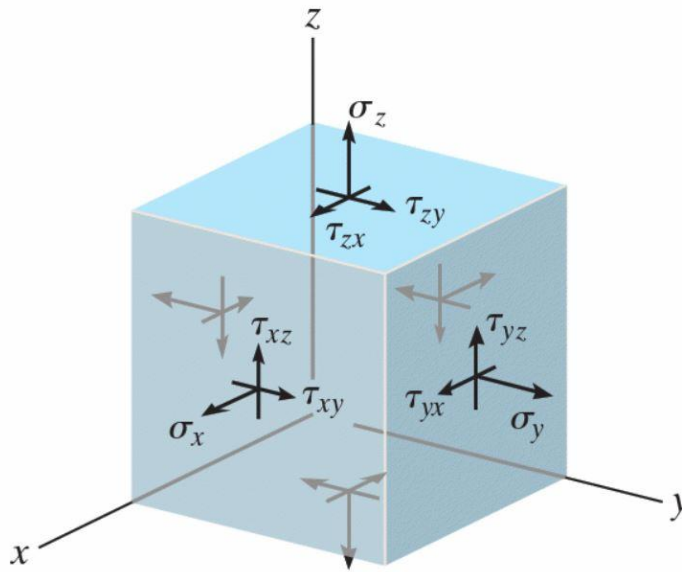
Figure 3. Stresses are characterized by three components acting on each face of the element. (Hibbeler 2018 p.41)

Therefore, shear stresses are presented as: $\tau = \sigma sin\vartheta = \frac{dFsin\vartheta}{dS}$, parallel to the chosen area.

Where the subscript rotation of z-axis specifies the direction of the selected area ΔS and other two axis reveal the surface along which the shear stress acts. Generally, shear stress is presented in form of τ_{ij} with the first index showing the direction of coordinate surface and the second one the direction of the shearing stress vector. Since stress is regarded as a vector, the magnitude of a stress is determined positive when it extends to the same direction as the coordinate axis (Silva 2006).

2.1.2. Stress matrix

A 3X3 matrix indicates components of a stress extending beneath different directions referring to Cartesian Coordinates. This method of arranging is called stress tensor or stress matrix. A stress can be separated into nine components forwards to different direction in coordinates. There nine components, however, can be arrayed in a matrix.

19

$$\sigma = \begin{bmatrix} \sigma_x & \tau_{xy} & \tau_{xz} \\ \tau_{xz} & \sigma_y & \tau_{yz} \\ \tau_{zx} & \tau_{yz} & \sigma_z \end{bmatrix} \tag{2-6}$$

Considering when stresses act on a surface which is inclined inside a structure, the components in reference directions can be expressed straight in equation with mathematical methodology, by inserting stress vectors (Silva 2006).

$$\begin{cases} T_x = x \cdot \sigma_x + y \cdot \tau_{yz} + z \cdot \tau_{zx} \\ T_y = y \cdot \sigma_y + x \cdot \tau_{xy} + z \cdot \tau_{zy} \\ T_z = z \cdot \sigma_z + x \cdot \tau_{xz} + y \cdot \tau_{yz} \end{cases} \tag{2-7}$$

Rearrange into the form of matrix:

$$\begin{bmatrix} T_x \\ T_y \\ T_z \end{bmatrix} = \begin{bmatrix} \sigma_x & \tau_{xy} & \tau_{xz} \\ \tau_{yx} & \sigma_y & \tau_{zy} \\ \tau_{zx} & \tau_{yz} & \sigma_z \end{bmatrix} \begin{bmatrix} x \\ y \\ z \end{bmatrix} \tag{2-8}$$

Where, T is the total stress vector (vector $\vec{T}$), σ_i is normal stress which is in right projection of the vector $\vec{T}$ and τ_{ij} is shear stress.

According to the reciprocity of shearing stresses (Silva 2006), a relationship among shear stresses across surfaces in variety can be acquired as below:

$$(\tau_{xy} = \tau_{yx}, \tau_{xz} = \tau_{zx}, \tau_{yz} = \tau_{zy}) \tag{2-9}$$

Thus, the normal stress can be defined in term of T as:
$$\sigma = x \cdot T_x + y \cdot T_y + z \cdot T_z$$

$$= x(x \cdot \sigma_x + y \cdot \tau_{yz} + z \cdot \tau_{zx}) + y(y \cdot \sigma_y + x \cdot \tau_{xy} + z \cdot \tau_{zy}) + z(z \cdot$$
$$\sigma_z + x \cdot \tau_{xz} + y \cdot \tau_{yz})$$

$$= x^2 \cdot \sigma_x + y^2 \cdot \sigma_y + z^2 \cdot \sigma_z = 2xy \cdot \tau_{xy} + 2xz \cdot \tau_{xz} + 2yz \cdot \tau_{yz} \tag{2-10}$$

Due to Pythagoras's theorem, the resultant stress vector is defined as (Silva 2006)

$$T^2 = \sigma^2 + \tau^2 \tag{2-11}$$

2.1.3. Transformation of stress

The general state of stress at the arbitrary point is determined by normal and shear stress's components. However, the most identical case which engineers ever encountered is not in three-dimension.

In Finite Element Analysis of beams, observation at cross-section is constantly adopted by engineers to clearly prove deflections, which calls forth a transformation of stress from 3D to 2D, in another word, to do plane stress analysis.
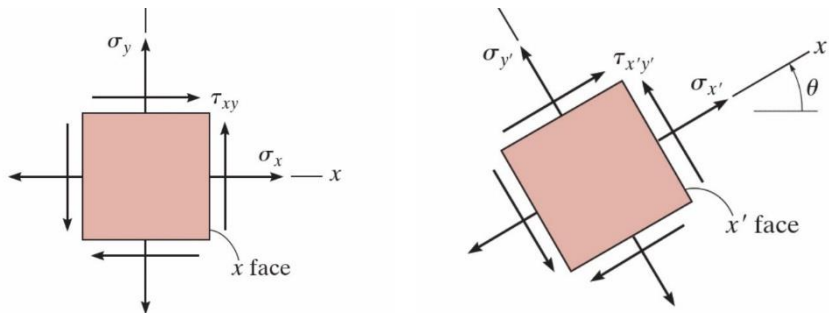
Figure 4. Plane stress presenting. (Hibbeler 2018 p.464)

The state of plane stress at the chosen point P is exclusively described by two normal stress components and one component of shear stress which are applied on the element (Hibbeler 2018). After an anti-clockwise rotation of the coordinate in an angle θ, forces which are applied on the former coordinate must be transformed to the new frame.

Hence, the matrix of stress converts:

$$\sigma = \begin{pmatrix} \sigma_x & \tau_{xy} & \tau_{xz} \\ \tau_{xz} & \sigma_y & \tau_{yz} \\ \tau_{zx} & \tau_{yz} & \sigma_z \end{pmatrix} \Rightarrow \sigma = \begin{pmatrix} \sigma_x & \tau_{xy} & 0 \\ \tau_{xz} & \sigma_y & 0 \\ 0 & 0 & 0 \end{pmatrix} \qquad (2\text{-}12)$$

By creating a free-body diagram on the segment (**Figure 5**), it is accessible to have basic equations which indicate normal and shear stresses upon the arbitrary surface in term of rotative angle.
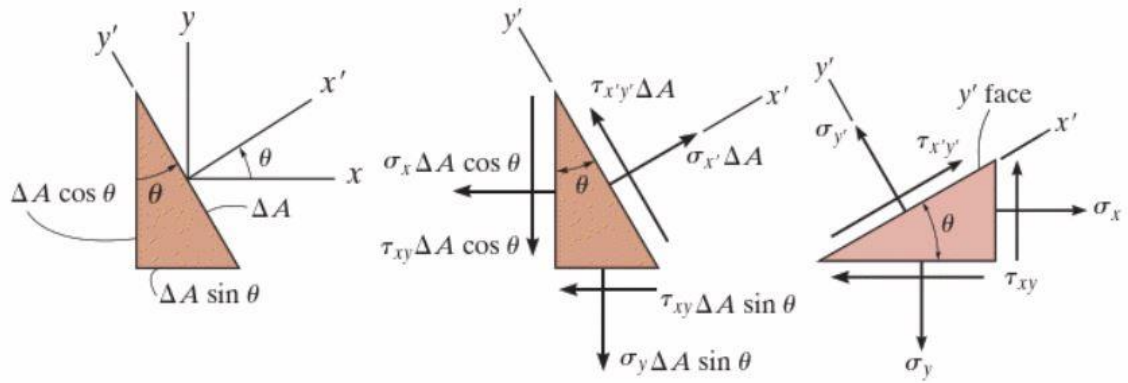
Figure 5*. Free-body diagram which shows equilibrium on the segment. (Hibbeler 2018 p.465)*

According to the resultant free-body diagram of the segment, to satisfy the equilibrium among physical quantities, normal σ_x' and shear stress τ_{xy}' after rotation can be acquired as (Hibbeler 2018):

$$\sigma_x' \cdot \Delta A - (\tau_{xy} \cdot \Delta A \sin\theta)\cos\theta - (\sigma_y \cdot \Delta A \sin\theta)\sin\theta - (\tau_{xy} \cdot \Delta A \cos\theta)\sin\theta - (\sigma_x \cdot \Delta A \cos\theta)\cos\theta = 0 \ ;$$

$$\sigma_x' = \sigma_x \cos^2\theta + \sigma_y \sin^2\theta + \tau_{xy} \cdot 2\sin\theta\cos\theta \ . \tag{2-13}$$

$$\tau_{xy}' \cdot \Delta A + (\tau_{xy} \cdot \Delta A \sin\theta)\sin\theta - (\sigma_y \cdot \Delta A \sin\theta)\cos\theta - (\tau_{xy} \cdot \Delta A \cos\theta)\cos\theta + (\sigma_x \cdot \Delta A \cos\theta)\sin\theta = 0 \ ;$$

$$\tau_{xy}' = (\sigma_y - \sigma_x)\sin\theta\cos\theta + \tau_{xy}(\cos^2\theta - \sin^2\theta) \ . \tag{2-14}$$

To simplify,

$$\sigma_x' = \frac{\sigma_x + \sigma_y}{2} + \frac{\sigma_x - \sigma_y}{2}\cos(2\theta) + \tau_{xy}\sin(2\theta) \tag{2-15}$$

$$\tau_{xy}' = -\frac{\sigma_x - \sigma_y}{2}\sin(2\theta) + \tau_{xy}\cos(2\theta) \tag{2-16}$$

Furthermore, by substituting θ with $(\theta + \frac{\pi}{2})$ (Protter, Murray, Morrey & Charles 1970), normal stress after rotation in y-axis direction can be determined as:

$$\sigma_y' = \frac{\sigma_x + \sigma_y}{2} - \frac{\sigma_x - \sigma_y}{2} \cos(2\theta) - \tau_{xy} \sin(2\theta) \qquad (2\text{-}17)$$

Apart from this, it is crucial to identify the orientation that makes the normal stress reach to the maximum value. (Hibbeler 2018) This is named as in-plane principle stress, which determines both maximum and minimum magnitudes of normal stress applied on an element. Equation (2-15) is differentiated respect to the rotation angle θ which leads to a result as (**Figure 6**):
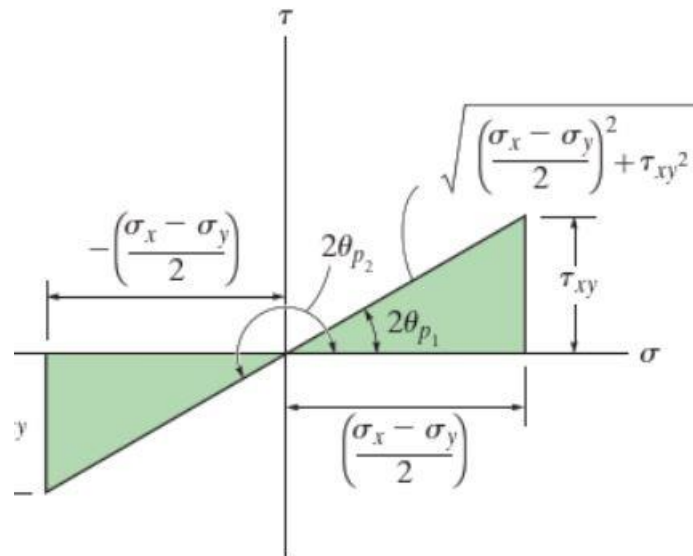
Figure 6. Critical value of normal stress. (Hibbeler 2018 p.471)

$$\frac{d\sigma_x'}{d\theta} = -\frac{\sigma_x - \sigma_y}{2}(2\sin 2\theta) + 2\tau_{xy} \cos(2\theta) = 0 \qquad (2\text{-}18)$$

By solving Equation (2-18), the orientation θ of the plane of the maximum and minimum normal stress is:

$$\tan 2\theta = \frac{2\tau_{xy}}{\sigma_x - \sigma_y} \qquad (2\text{-}19)$$

$$\theta = \frac{1}{2}\tan^{-1}\left(\frac{2\tau_{xy}}{\sigma_x - \sigma_y}\right) \qquad (2\text{-}20)$$

23

Where the function respect to θ possesses two roots, which are $\theta_1 = \theta$ and $\theta_2 = \theta + \frac{\pi}{2}$ due to the trigonometric function. Therefore, the corresponding normal stresses are presented as (Hibbeler 2018):

$$\sigma_{1,2} = \frac{\sigma_x + \sigma_y}{2} \pm \sqrt{\left(\frac{\sigma_x - \sigma_y}{2}\right)^2 + \tau_{xy}^2} \qquad (2\text{-}21)$$

By using the analogous method (**Figure 7**), the maximum shear stress is acquired as (Hibbeler 2018):

$$\frac{d\tau'_{xy}}{d\theta s} = -\frac{\sigma_x - \sigma_y}{2}(\sin 2\theta s) + \tau_{xy}\cos(2\theta s) = 0 \qquad (2\text{-}22)$$
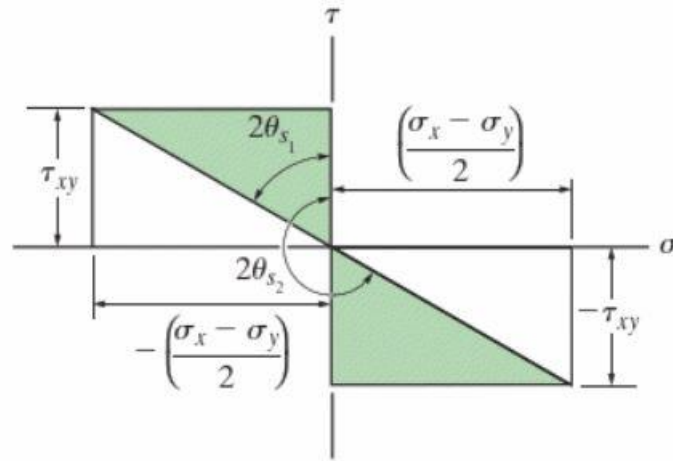
Figure 7. Critical value of shear stress. (Hibbeler 2018 p.472)

Hence,

$$\tau_{\max in-plane} = \sqrt{\left(\frac{\sigma_x - \sigma_y}{2}\right)^2 + \tau_{xy}^2} \qquad (2\text{-}23)$$

2.1.4. Strain

Strain is the physical quantity to express deformation of a body when a force is applied on. In general, the deformation is not uniform throughout the body. Thus, the change in geometry of any segment aligned within the frame may vary substantially along the length (Hibbeler 2018). Temperature variation or similar phenomena is also a possible elicitation of deformation. Analogously,

strain tensor is defined by same mathematical characteristics as the stress tensor under the validity of the continuum hypothesis (Silva 2006).

2.2. Two types of beam deflection

Generally, two delegative sorts of beam deflection commonly discussed are put in contrast which indicated visual disparities on angles at the end of ingredients, called Euler-Bernoulli Beams and Timoshenko Beams, respectively. A beam is defined as a configuration where one of its dimensions is much larger than the other two. The axis of the beam is defined along that longer dimension and a cross-section normal to this axis is hypothesized to smoothly vary along the span or length of the beam (Bauchau & Craig 2009 p.173). Civil engineering structures constantly are comprised of an assembly or grid of beams with cross-sections underneath shapes such as T's or I's. Machine parts also are beam-like structures: lever arms, shafts and so forth. Eventually, several aeronautical structures such as wings and fuselages can also be treated as thin-walled beams (Bauchau & Craig 2009).

2.2.1. Euler-Bernoulli Beam Theory

Euler-Bernoulli Beam Theory is universally regarded as classical beam theory, which is a simplification of the linear theory of elasticity. This theory provides resolution to calculating load-carrying and deflection characteristics of beams. In addition, Euler-Bernoulli Theory underestimates the range of deflection at the end of the beam (due to shear strength effects).

By elements analysis, considering the objective beam is split into numerous uniform-size cubes, arrayed perpendicular to the neutral axis (shown as *Figure 8*). There is a load P upwards at the vertex of the beam which provides a moment of bending.
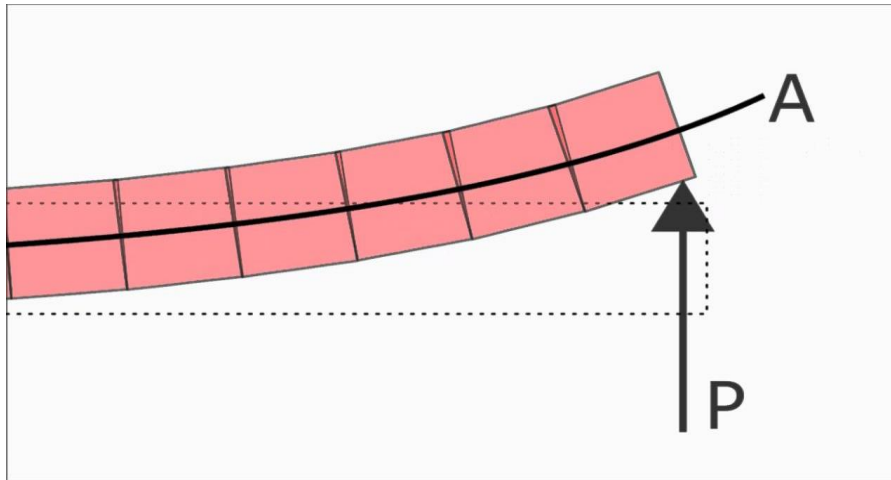
Figure 8*. Euler-Bernoulli Beam Theory. (accessed at 10/12/2019)*
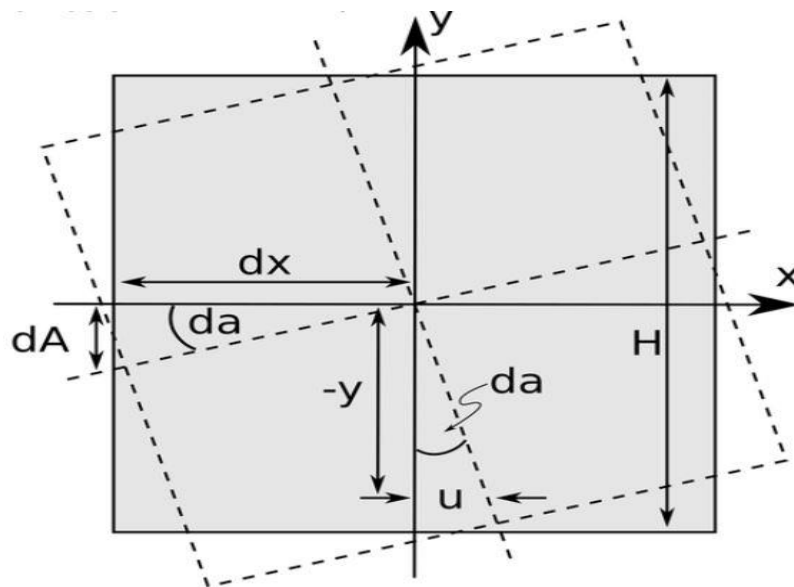
Figure 9*. Every single square remains the shape after bending. (accessed at 10/12/2019)*

The trait of Euler-Bernoulli Beam Theory, consequently, is summarized as any plane vertical to the neutral axis before bending will remain the same after the bending. The edge of the beam remains as 90 degrees throughout the deformation. The Euler–Bernoulli Equation describes the relationship between the beam's deflection and the applied load is as shown below (Gere & Timoshenko 1997):

$$\frac{d^2}{dx^2}\left(EI\frac{d^2w}{dx^2}\right) = q \qquad (2\text{-}24)$$

Where E is elastic modulus, I is the second moment of inertia, w(x) describes the deflection of the beam in the vertical direction at some position x. q is a distributed load, in other words a force per unit length (Gere & Timoshenko 1997).

2.2.2. Timoshenko Beam Theory

Timoshenko Beam Theory is a unique case apart from Euler-Bernoulli Theory. In comparison, Euler-Bernoulli Theory does not involve the correction for rotary inertia or the correction of shear stress which means there will be a different stress distribution in transverse direction when either a torsion or shear moment occurs on the beam, since the rotation from shear deformation between the cross section and bending line is considered negligible under Euler-Bernoulli Beam Theory. Adversely, Timoshenko Theory considers both which further demonstrates that the correction of shear is approximately 4 times greater than that of rotatory inertia.
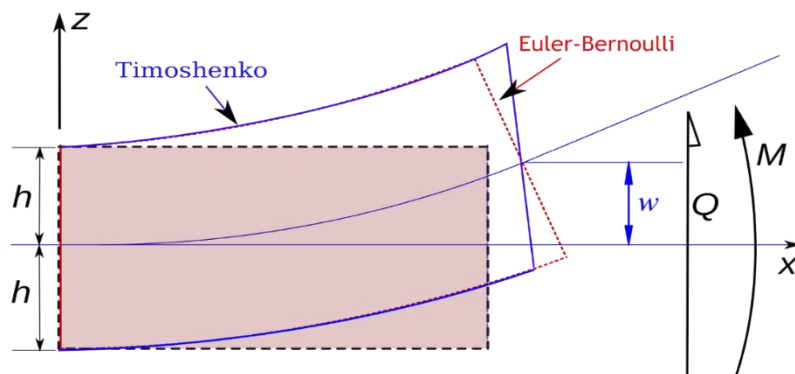
Figure 10. Comparison between Euler-Bernoulli and Timoshenko theory. (accessed at 10/12/2019)

The visual disparity between two types of beam theories is whether the shape of the end changes after bending (***Figure 10***). There is a strain which exists at the top and the bottom of the end. Consequently, this induces a deformation of shear. The angle at the vertex is no longer 90 degrees by contrast to the situation in Euler-Bernoulli Theory.

Beams which are either short or have colossal deflections are better modelled with Timoshenko theory. It includes that the added mechanisms of deflection effectively lower the stiffness of the beam. As a result, a large deflection under a static load and lower predicated eigenfrequencies occurs within a set of boundary conditions since by contrast, the wavelength becomes shorter when frequency climbs. Therefore, the distance between opposing shear forces decouples (Timoshenko 1922).

Likewise, in the static Timoshenko Beam Theory without axial effect, the relevant equation is governed as (Gere & Timoshenko 1997):

$$\frac{d^2}{dx^2}\left(EI\frac{dw}{dx}\right) = q \tag{2-25}$$

Nevertheless, Timoshenko Beam Theory for static cases is equivalent to Euler-Bernoulli Beam Theory when it caters for the condition below (Timoshenko 1922):

$$\frac{EI}{kL^2AG} \ll 1 \tag{2-26}$$

Where k is Timoshenko shear coefficient depending on the geometry. Normally, k= 5/6 for a rectangular section. L is the length of beam. A is the cross-section area and G means the shear modulus.

2.3. Discrepancies between solid and beam elements

Elements are consistently categorized in three main prevalent types which are solid, shells and line. Solid element is the most common type whose example can be linear tetrahedral. On the other side, one of the representatives of line element is beam. Generally, differences between solid and beam elements being applied throughout structural analysis can be distinguished via two aspects: the deviation on degree of freedom as well as the length-to-span ratios.

2.3.1. Degree of freedom

Degree of freedom is a parameter which describes possibilities to mobilize a 3D object in directions along the axis under coordinate. To illustrate, a cube under a Cartesian coordinate possesses six means of degree of freedom since it can be not only moved along X, Y or Z axis but can be rotated about three axes as well. In finite elements, the degree of freedom is controlled at the corner nodes. It declares three main purposes which identifies the locations where loads are applied, nodes where the solver reports result back to the monitor and nodes where the movement is constrained (Ellobody, Feng & Young 2013).

Nevertheless, disparities occur when it comes to comparing differences of what the concept support between beam elements and solid elements. Technically, beam elements support the definition which allows all six degrees of freedom.
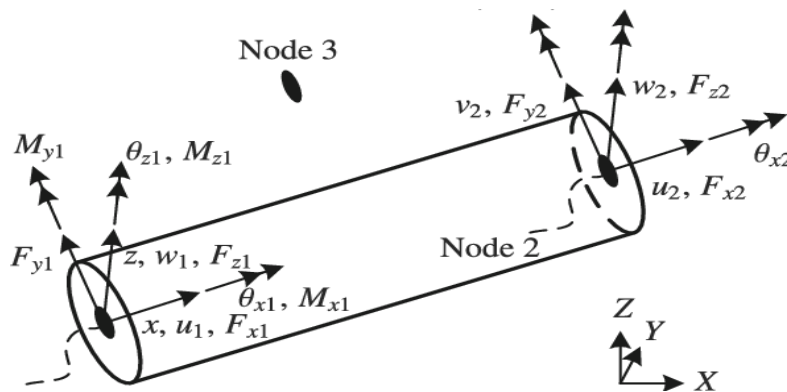
Figure 11. Six degrees of freedom of 3D beam elements between two nodes, accessed 26/02/2020.

Whereas, adversely, degrees of freedom in rotation directions are not involved in solid mechanics. To be specific, when a beam element is treated, the console can control the object move in either translational or rotational way (Ellobody, Feng & Young 2013). However, it is not allowed to control the solid elements in rotational direction.
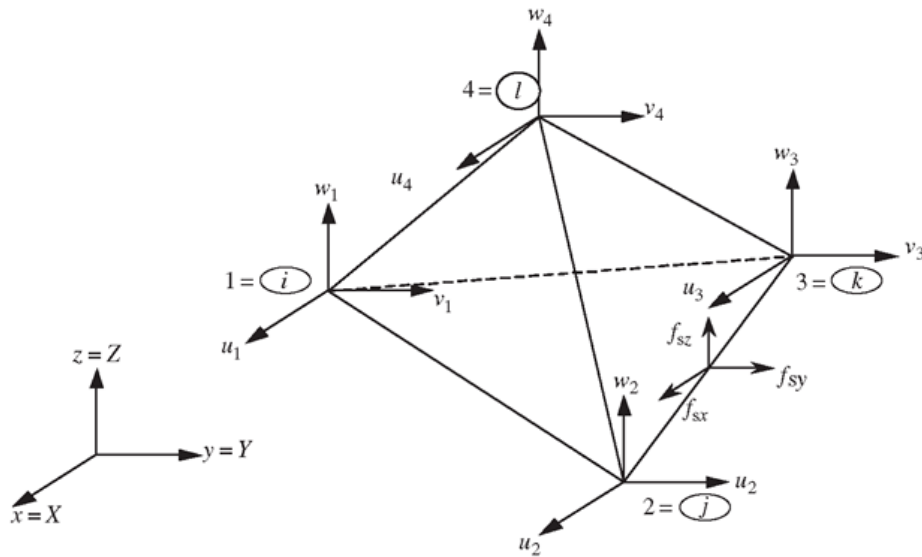
Figure 12. *Three degrees of freedom of a 3D solid element, accessed 26/02/2020.*

2.3.2. Length-to-span ratios

Apart from differing by degree of freedom, another trait which can reveals the discrepancy is length-to-span ratios. Beam elements are defined to be a single line representing the path of a beam with the cross-sectional moment of inertia, whereas solid elements are representing the entire geometry.

By FEA testing and analytical calculations on deflection and stress (shown in **Table 1** and **Table 2**), differences between solid and beam elements are concluded as that Beam elements offer obvious accuracy for deflection below length-span ratios of 8:1. Solid elements indicate analogous accuracies to beams for deflections but higher errors for stresses. Reducing the solid-element mesh size would compensate for this error.

Table 1. Results of FEA testing and calculations for deflection which shows the differences between solid and beam elements by length-to-span ration. (GoEngineer 2016, accessed on 27 Feb. 2020)

Deflection					
Beam Length (mm)	Analytical (mm)	Beam (mm)	% error	Solid (mm)	% error
15	0.0011	0.0014	20.51%	0.0006	-94.09%
20	0.0026	0.0030	12.69%	0.0030	15.13%
30	0.0087	0.0093	6.07%	0.0094	6.89%
40	0.0207	0.0215	3.52%	0.0215	3.65%
50	0.0404	0.0414	2.27%	0.0413	2.18%
60	0.0698	0.0710	1.58%	0.0708	1.36%
70	0.1109	0.1122	1.15%	0.1119	0.88%
80	0.1656	0.1671	0.92%	0.1666	0.62%
90	0.2357	0.2374	0.70%	0.2367	0.41%
100	0.3234	0.3252	0.57%	0.3242	0.26%
120	0.5588	0.5610	0.40%	0.5594	0.11%
140	0.8873	0.8899	0.29%	0.8875	0.02%
160	1.3245	1.3280	0.26%	1.3240	-0.04%
180	1.8858	1.8890	0.17%	1.8850	-0.05%
200	2.5869	2.5910	0.16%	2.5850	-0.07%

Table 2. Results of FEA testing and calculations for stress which shows the differences between solid and beam elements by length-to-span ration. (GoEngineer 2016, accessed on 27 Feb. 2020)

Stress					
Beam Length (mm)	Analytical (MPa)	Beam (MPa)	% error	Solid (MPa)	% error
15	15.28	15.28	0.01%	11.71	-30.48%
20	20.37	20.37	-0.01%	18.98	-7.33%
30	30.56	30.56	0.01%	28.54	-7.07%
40	40.74	40.74	-0.01%	40.36	-0.95%
50	50.93	50.93	0.00%	50.12	-1.62%
60	61.12	61.12	0.01%	59.83	-2.15%
70	71.30	71.3	0.00%	67	-6.42%
80	81.49	81.49	0.00%	76.45	-6.59%
90	91.67	91.67	0.00%	90.17	-1.67%
100	101.86	101.9	0.04%	100.3	-1.55%
120	122.23	122.2	-0.03%	116.4	-5.01%
140	142.60	142.6	0.00%	140.7	-1.35%
160	162.97	163	0.02%	156.9	-3.87%
180	183.35	183.3	-0.03%	180.9	-1.35%
200	203.72	203.7	-0.01%	197.4	-3.20%

2.3.3. Merits and demerits of using beam elements

Consistently, beam elements are more widely applied than solid elements during Finite Element Analysis on structures. However, there are abundant merits of using beam elements rather than solid elements (Clough 1960). For instance, the formulation of beam elements is straightforward, which facilitate the calculation process with a precise result. Beam elements are trivial for meshing which diminish the deviation which comes from mesh refinement in stress concentration regions. Another advantage is that the analysis process is curtailed. Moreover, beam elements can handle more complex structures without mesh. Hence, it is available to acquire various output variables including section forces and moments. Point load will not have much influence on stress singularity.

On the contrary, there are also existing some demerits of using beam element instead of solid elements (Clough 1960). Significant simplifications are induced when beam elements are used. When beam elements are introduced to simulations, not all stress components extending to different directions as well as distribution through the thickness can be captured.

3. METHOD

Modelling elements are sketched and simulated by Comsol Multiphysics to indicate that how deflection of the beams differs under two types.

Solid mechanics as well as beam modulus are added into study to create comparison showing different effects. The function of solid mechanics is to define the quantities and features for stress analysis, general linear and nonlinear solid mechanics for the displacements. It enables large deformation with geometric nonlinearity and follower loads. On the contrary, beam modulus is exerted due to the strength of depiction of sectional properties such as second moment of inertia. Beam modulus, nevertheless, can also simulate frame structures, both in plane and in 3D. Synchronously, it can be coupled with other element types, such as for analysing reinforcements of solid and shell structures. To make the comparison of deflections more specific and concrete, beams are drawn variously with two different sections (normal beams with rectangular cross-section and 'I' beam).

3.1. Material selection

Table 3: *Mechanical property of aluminium (Comsol Material Library).*

Density	rho	2700[k...	kg/m³
Young's modulus	E	70e9[Pa]	Pa
Poisson's ratio	nu	0.33	1
Relative permeability	mur_i...	1	1
Heat capacity at constant p...	Cp	900[J/(...	J/(kg·...

Young's modulus is $E = 70GPa$ with Poisson's ratio of 0.33

To cater for the primary orientation of this thesis, which is to compare the differences between deflections underneath Euler-Bernoulli and Timoshenko types, a material with sufficient elasticity and high rigidity ought to be applied to the models to undertake massive quantity of loads in the simulation. Sharpe deflections required to the observation. Hence, aluminium is selected as the material which is applied on both moulds.

3.2. Finite Element Analysis in Comsol

The definition of Finite Element Analysis is the simulation of any physical phenomenon using the numerical technique called Finite Element Method (FEM).

Nodes and elements are identical backbones of Finite Element Analysis used in Comsol. When a model is divided into several small parts, they are knitted together by characteristic points which are called nodes. Each element shares a common node in adjacent. By contrast, mesh is defined by connecting nodes to form a net-shape system which is covered full of the surface of the objectives. Meshed are crucial for precise result acquisition. By creating a mesh plot, it is visible to inspect on defects of the entities of the mould and to understand where low-quality elements are positioned. Constantly, mesh is widely applied by great many of computational software.

3.3. Comsol modelling

To differentiate demonstrations of Euler-Bernoulli Beam Theory and Timoshenko Beam Theory, it is necessary to create beams with cross sections of three different geometries. According to the corresponding theory, beams designed for simulations are in cross section of square (thick), rectangular (thin) and I-shape. To diminish the errors during the simulation due to dimensions of the beams, beams are designed underneath same dimensions of width as 0.08 meters and varies on height. All beams are designed extending in depth direction by 0.6 meters.

Square cross-sectional

In the first occasion, the beam is designed as a thick beam with a square cross section of dimension of 0.08 meters x 0.08 meters, which satisfy the Timoshenko Beam Theory.

Rectangular cross-sectional

The second beam is sketched with a rectangular cross section which is thinner than the beam designed for the first case. The dimension is 0.08 meters x 0.03 meters. Euler-Bernoulli Beam Theory will be displayed by the beam with thinner cross section.

6- beam

In the third occasion, I-beam is used to investigate how both two beam theories differ on beams with a different shape. The dimensions of I beam retain the same with the dimensions in early two occasions. The thickness of web part is 0.02 metres.

3.4. Loading

In the process of simulation, load is applied in different occasions with different magnitudes to imitate the effects on deformation of the domain due to surface loading as well as compression along the depth and torsions. The emergence of the deformation is accounted of bending moment and torque as soon as the load is applied on domain. Since beam element is consisted of six degrees of freedom, it is straightforward to observe the deformation of the beam in rotational direction when a force is applied along depth.

3.4.1. Bending

In the first occasion, shear force is used to induce the deformation to the beams. A distributed load is applied perpendicularly to the surface which is uniformly distributed with a magnitude of 5000 N/m. The load, consequently, is 3000 N.
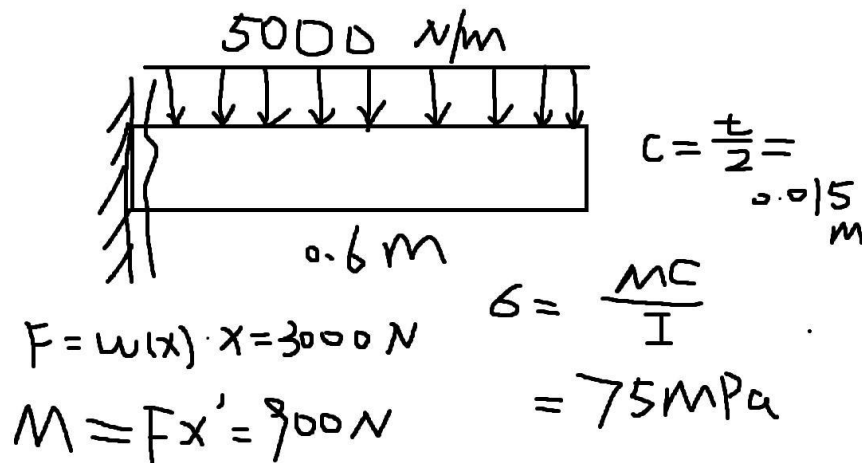

Figure 13. Free-body diagram of the surface load occasion, gao jie, 27/02/2020.

Therefore, there will be a curvature of cantilever beam occur due to the bending moment in the respect of the free length under the distributed load elongating along the length of the beam.
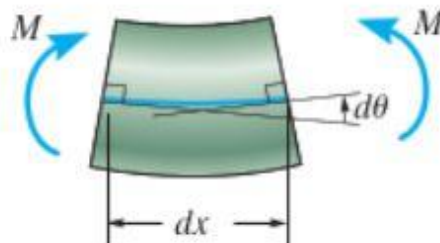

Figure 14. Deformation of an element under bending moment. (Hibbeler 2018 p.629).

In consequence, the bending moment from the shear force which is acting at the boundary edge of the beams can be calculated as (Bauchau & Craig 2009):

$$M_{bending}(x) = Fx = 900\ N \cdot m \qquad (3\text{-}1)$$

Where,

$M_{bending}(x)$ is the bending moment.

F is the total load at surface.

x is the distance between the boundary edge and the point where the load is applied on the surface.

Since the beam is under a uniform distributed load which is applied vertically at the surface, the formulation of obtaining the maximum stress and displacement are presented in **Figure 15** below:
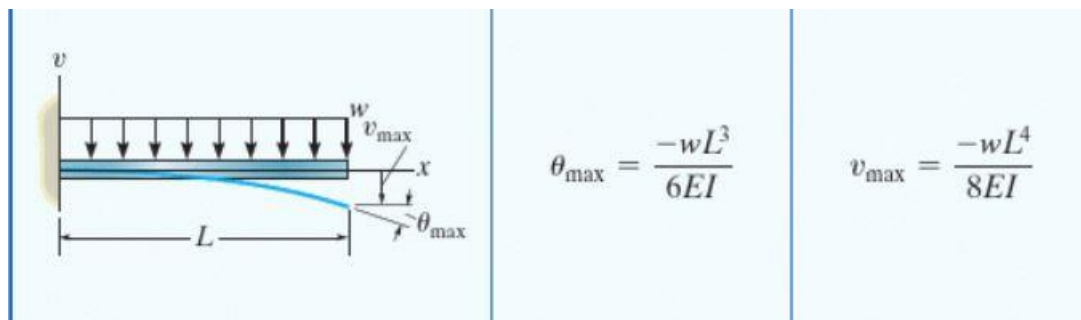
Figure 15. The angle of deformation and maximum displacement of a beam under a distributed load. (Hibbeler 2018 p.830).

Hence, by inserting magnitudes, the maximum displacement is obtained as: $t_{max} = -6.45\ mm$. Moreover, the maximum normal stress in the member is calculated as (Hibberler 2018 p. 313):

$$\sigma_{max} = \frac{Mc}{I} = 75\ MPa \qquad (3\text{-}2)$$

Where,

c   is perpendicular distance from the neutral axis to a point farthest away from the neutral axis.

3.4.2. Axial load along direction of depth

In the second occasion, an axial load is directly applied along the direction of depth, which is perpendicular to the cross section. Therefore, the normal stress which is acting at the cross section of the beams can be calculated as (Bauchau & Craig 2009):

$$\sigma = \frac{P}{A} \tag{3-3}$$

Furthermore, the strain due to the axial load is determined as:

$$\epsilon = \frac{PL}{AE} \tag{3-4}$$

Generally, due to the assumptions of Euler-Bernoulli Beam Theory, it is available to imitate the situation when the beam is subjected to distributed axial loads (Bauchau & Craig 2009). There are three fundamental assumptions which are concluded from Euler-Bernoulli Beam Theory. The first assumption states that the cross section of the beam is un-deformable in the selected plane. In another word, the cross section is infinitely rigid. The second assumption suggests that the cross section is able to deform and will retain plane after deformation, which implies an axial displacement region which consists of a rigid domain translation and two rigid domain rotations as well. The third assumption states that the cross section remains normal to the neutral axis of the beam after deformation (Bauchau & Craig 2009) (**Figure 17**).
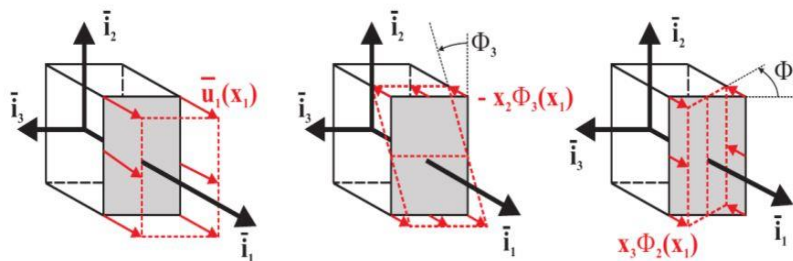
Figure 16. Decomposition of axial displacement region. (Bauchau & Craig 2009 p. 175)

3.4.3. Torsion

In the third occasion, a torque is applied to demonstrate the degrees of freedom od beam elements in rotational direction. A torsion T is applied at the cross-section surface which creates a shear stress at the transverse level to make the beam twist in a certain angle.
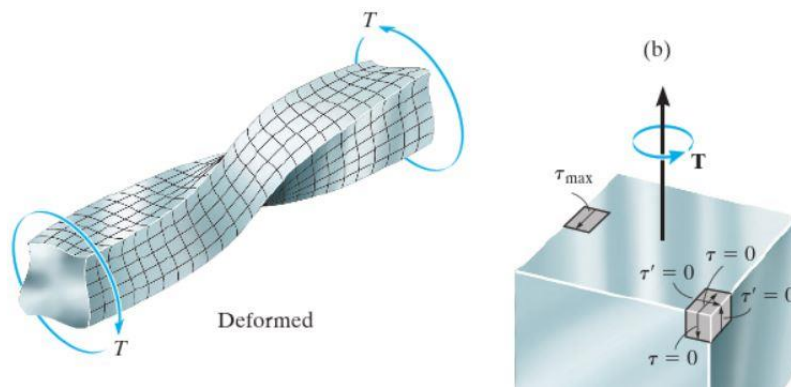
Figure 17. FBD of torsion of a noncircular beam (Hibbeler 2018 p.247).

The corresponding formula of torsion and twisted angle, therefore, is given as:

Square:

Table 4. The maximum shear stress and twist angle of a square cross section. (Hibbeler 2018 p.248)

Shape of cross section	τ_{max}	ϕ
Square	$\dfrac{4.81\ T}{a^3}$	$\dfrac{7.10\ TL}{a^4 G}$

Where T is torsion, L is the depth of the beam, G is the shear modulus of the material and Ø is the angle of twist.

Rectangular:

The constant in torsion equations of a rectangular cross section depends on the ratio of width over height (Ugural & Fenster 1975).
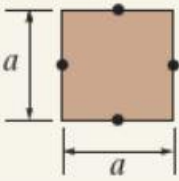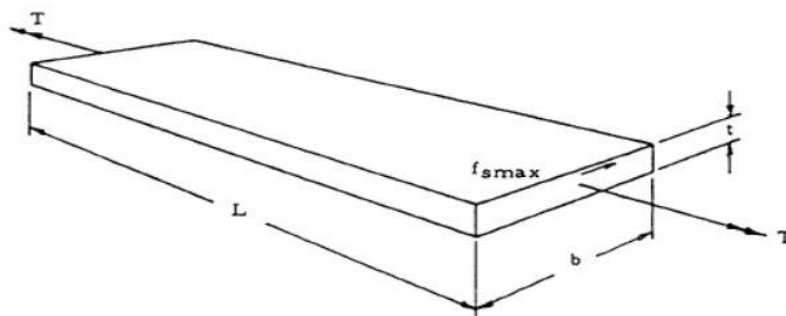

Figure 18. Torsion of rectangular cross section. (accessed from Engineering Library at 27/02/2020)

The maximum stress of a rectangular beam occurs at the center of the long side and is given by:

$$\tau_{max} = \frac{T}{\alpha b t^2} \tag{3-5}$$

Where, α is a relevant constant, b is the width of beam and t is the thickness.

Therefore, the angle of twist of a rectangular beam is given as:

$$\emptyset = \frac{TL}{\beta b t^3 G} \tag{3-6}$$

Where α and β are given in **table 5** as:

Table 5. Constant of torsion Equations (3-7) and (3-8) (Urugal, A.C & Saul K. Fenster 1975).

b/t	1.00	1.50	1.75	2.00	2.50	3.00	4	6	8	10	∞
α	0.208	0.231	0.239	0.246	0.258	0.267	0.282	0.299	0.307	0.313	0.333
β	0.141	0.196	0.214	0.229	0.249	0.263	0.281	0.299	0.307	0.313	0.333

6- beam:
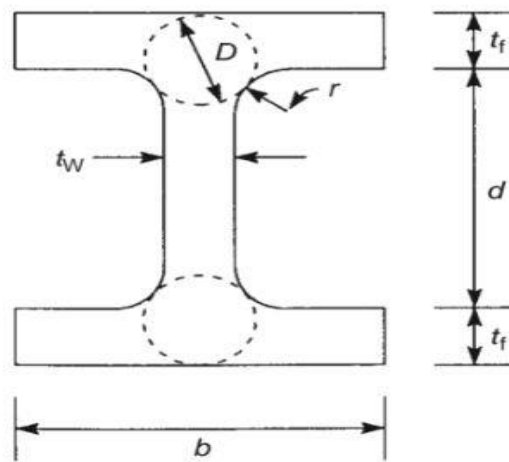
Figure 19. Torsion of a I-section beam, (Megson 2005 p. 292)

According to the diagram **Figure 20**, the maximum shear stress of a I-section beam is summarized as (Megson 2005):

$$\tau_{max} = \frac{G\emptyset c}{L} \tag{3-7}$$

Where,
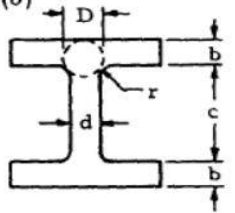
$$c = \frac{D}{1 + \frac{\pi^2 D^4}{16A^4}}\left[1 + (0.118 \ln\left(1 - \frac{D}{2r}\right) - \frac{0.238D}{2r}) \tanh\frac{2\emptyset}{r}\right]$$

Where,

A is the area of the cross section.

41

Moreover, the angle of twist of the I-section beam is given as **Table 6**.

Table 6. The angle of twist of I-section beam due to torsion (engineer-inglibrary.org. (n.d.). Beam Torsion | Engineering Library, accessed 27 Feb. 2020).

(6) I section, flange thickness. r = fillet radius D = diameter of largest inscribed circle $t = b$ if $b < d$, $t = d$ if $d < b$, $t_1 = b$ if $b > d$, $t_1 = d$ if $d > b$	$$\theta = \frac{TL}{G(2K_1 + K_2 + 2aD^4)}$$ where $$K_1 = ab^3 \left[\frac{1}{3} - 0.21\frac{b}{a}\left(1 - \frac{b^4}{12a^4}\right) \right]$$ $$K_2 = \frac{1}{3}cd^3$$ and $$a = \frac{t}{t_1}\left(0.15 + 0.1\frac{r}{b}\right)$$

4. RESULTS

4.1. Mathematical calculations

The cross section of the specimens lies in x, y axial direction and the specimens extend in z axial direction. According to the given dimensions, the cross-sectional area of rectangular beam and I beam is regarded as $A_{rectangular}$ and A_I for respective.

Hence, in the first occasion,

$$A_{square} = b \times h = 0.08 \times 0.08 = 6.4 \times 10^{-3} \; m^2 \qquad (4\text{-}1)$$

Furthermore, the moment of inertia of the cross-sectional area about neutral axis each is calculated as:

$$I_{square} = \frac{1}{12}bh^3 = \frac{1}{12} \times 0.08 \times 0.08^3 = 3.41 \times 10^{-6} \; m^4 \qquad (4\text{-}2)$$

In the second occasion, the area of rectangular section is calculated as:

$$A_{rectangular} = b \times h = 0.08 \times 0.03 = 2.4 \times 10^{-3} \; m^2 \qquad (4\text{-}3)$$

Therefore, the moment of inertia of the cross section is defined as:

$$I_{rectangular} = \frac{1}{12}bh^3 = \frac{1}{12} \times 0.08 \times 0.03^3 = 1.8 \times 10^{-7} \; m^4 \qquad (4\text{-}4)$$

In the third occasion, the I-section beam is designed under two different thicknesses by comparison to indicate the disparity of two beam theories during the simulation. For thin beam, which satisfy Euler-Bernoulli Beam Theory, the related property is given as:

$$A_{I-beam} = \Sigma A = 1.8 \times 10^{-3} \; m^2 \qquad (4\text{-}5)$$

According to the formula which indicates the moment of inertia of I beam (Hibbeler 2018, p316), the parameter related is:

$$I_{I-beam} \quad = \sum \hat{I} + Ad^2 = 2\left[\frac{1}{12}(0.08\,m)(0.01\,m)^3 + 0.08\,m \times 0.01\,m \times\right.$$

$$(0.01\,m)^2\left.\right] + \left[\frac{1}{12} \times 0.02\,m \times (0.01\,m)^3\right] = 1.75 \times 10^{-7}\,m^4 \qquad (4\text{-}6)$$

Likewise, for thick beam, which satisfy Timoshenko Beam Theory, the related property is given as:

$$A_{I-beam} = \sum A = 2.8 \times 10^{-3}\,m^2 \qquad (4\text{-}5)$$

$$I_{I-beam} = \sum \hat{I} + Ad^2 = 2\left[\frac{1}{12}(0.08\,m)(0.01\,m)^3 + 0.08\,m \times 0.01\,m \times\right.$$

$$(0.035\,m)^2\left.\right] + \left[\frac{1}{12} \times 0.02\,m \times (0.06\,m)^3\right] = 2.34 \times 10^{-6}\,m^4 \qquad (4\text{-}6)$$

To make mathematical calculation of related parameters, for instance, in the occasion of section **3.4.1**, a uniform load distribution is applied perpendicular to the top surface of the beam in negative direction with a magnitude of 5000 N/m.

To demonstrate, for the rectangular cross-sectional beam: the surface load perpendicular to the beam is:

$$F = q(x)x = 5000 \times 0.6\,N = 3000\,N$$

The corresponding bending moment, consequently, is determined by Equation (3-1) as:

$$M_{bending}(x) = Fx = 3000 \times 0.3 = 900\,N \cdot m$$

The maximum normal stress is obtained as:

$$\sigma_{max} = \frac{M_{bending}(x)c}{I} = \frac{900 \times 0.015}{1.8 \times 10^{-7}}\,Pa = 75 \times 10^6\,Pa = 75\,MPa$$

The equation above induces a bending deformation. Referring to **Table 3. Mechanical property of aluminium,** the Young's modulus of aluminium is $E = 70GPa$. Inserting the related value of properties back to Equation (3-2). The displacement of deflection is determined as:

$$t_{max} = -\frac{q(x)L^4}{8EI} = 6.45 \; mm$$

Afterwards, anticipating that the axial load is applied as 1000 N in the occasion of **3.4.2**, the normal compressive stress at the cross section is determined via Equation (3-5) as:

$$\sigma = \frac{P}{A_{square}} = 0.16 \; MPa$$

The strain, likewise, is obtained via Equation (3-6) as:

$$\epsilon = \frac{PL}{A_{square}E} = \frac{1000 \times 0.6}{6.4 \times 10^{-3} \times 70 \times 10^9} \; m = 1.34 \times 10^{-6} \; m$$

In the occasion of section **3.4.3**, where torque is hypothesized as $T = 500 \; N \cdot m$, the maximum stress occurs at the square-sectional beam. The shear modulus of silicon is determined by Young's Modulus and Poisson's Ratio as $G = \frac{E}{2(1+v)} = 26.32 \; GPa$ (Bauchau & Craig 2009) and the related twist angle are determined as:

$$\tau_{max} = \frac{4.81 \times 500}{0.08^3} \; Pa = 4.7 \; MPa$$

$$\emptyset = \frac{7.1 \times 500 \times 0.6}{0.08^4 \times 26.32 \times 10^9} \; rad = 1.976 \times 10^{-3} \; rad$$

Hence, to summarize the consequences of all cases in the tables below:

Table 7. Mathematical results of surface load situation.

Surface load	Maximum normal stress (MPa)	Maximum displacement (mm)
Rectangular beam (0,08 m*0,03 m)	75	6,45
Square beam (0,08 m*0,08 m)	10,55	0,339
I-beam (0,03 m thick)	77,14	6,61
I-beam (0,08 m thick)	15,4	0,495

Table 8. Mathematical results of axial load situation.

Axial load	Maximum normal stress (MPa)	Maximum displacement (mm)
Rectangular beam (0,08 m*0,03 m)	0,42	3,57E-03
Square beam (0,08 m*0,08 m)	0,16	1,34E-03
I-beam (0,03 m thick)	0,56	4,78E-03
I-beam (0,08 m thick)	0,36	3,06E-03

Table 9. Mathematical results of torsion situation.

Torsion	Maximum normal stress (MPa)	Twist angle (rad)
Rectangular beam (0,08 m*0,03 m)	26,7	0,021
Square beam (0,08 m*0,08 m)	4,7	1,98E-03
I-beam (0,03 m thick)	77,14	0,661
I-beam (0,08 m thick)	15,4	4,27E-03

4.2. Simulation by Comsol

Mesh results from the tetrahedral mesh size of 'extra fine' setup which specify the element size as well as relative tolerance value.
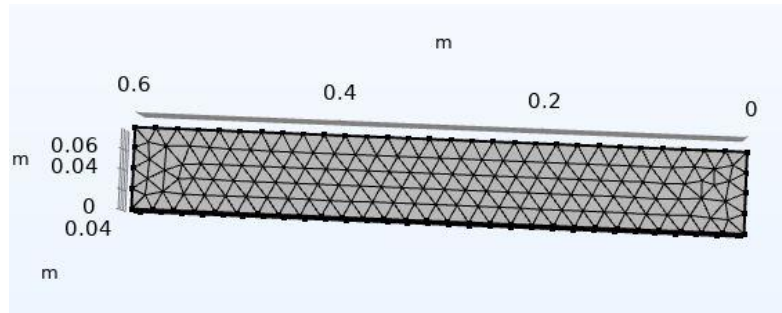

*Figure **20**. Extra fine meshed square cross-sectional elements, gao jie, accessed 16/03/2020.*

Objectives are consisted of numerous meshed elements of designed beams in sections above, which are square cross-sectional, rectangular cross-sectional and I-beam. Euler-Bernoulli and Timoshenko formulation are set as counterparts.

Moreover, it is necessary to compare different results by applying beam modulus analysis and solid mechanics analysis on beams, which makes the disparities on the concept of degree of freedom between two nodes more concrete to see.

4.2.1 Bending simulation

Rectangular beam:

Firstly, underneath solid mechanics analysis, a distributed load of 5000 N/m is applied uniformly at the surface of the beam. The beam element will bend due to the load. In addition, labels which contain related information such as values of either maximum or minimum stresses among stress distribution as well as titles defining diagrams are plotted after running the computation. For instance, **Figure 21** explains the reaction of thin beam under the uniform load distribution.

It is coloured to differ the contour of principal stress of normal stress in unit of MPa.
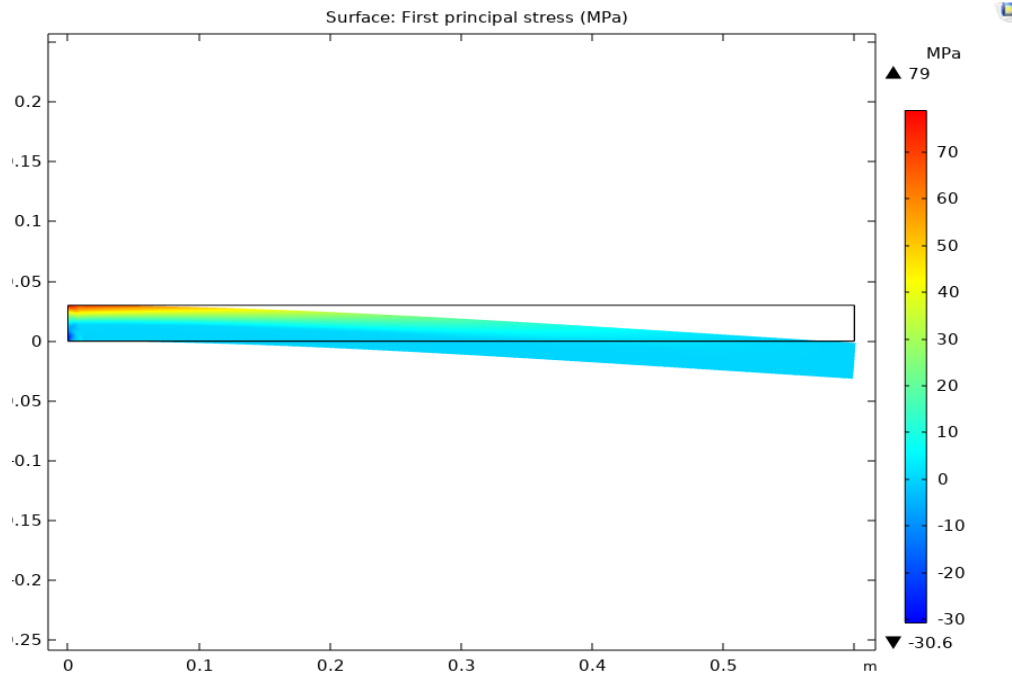

*Figure **21**. Maximum normal stress of rectangular beam due to bending, solid mechanics, gao jie, accessed 19/03/2020.*
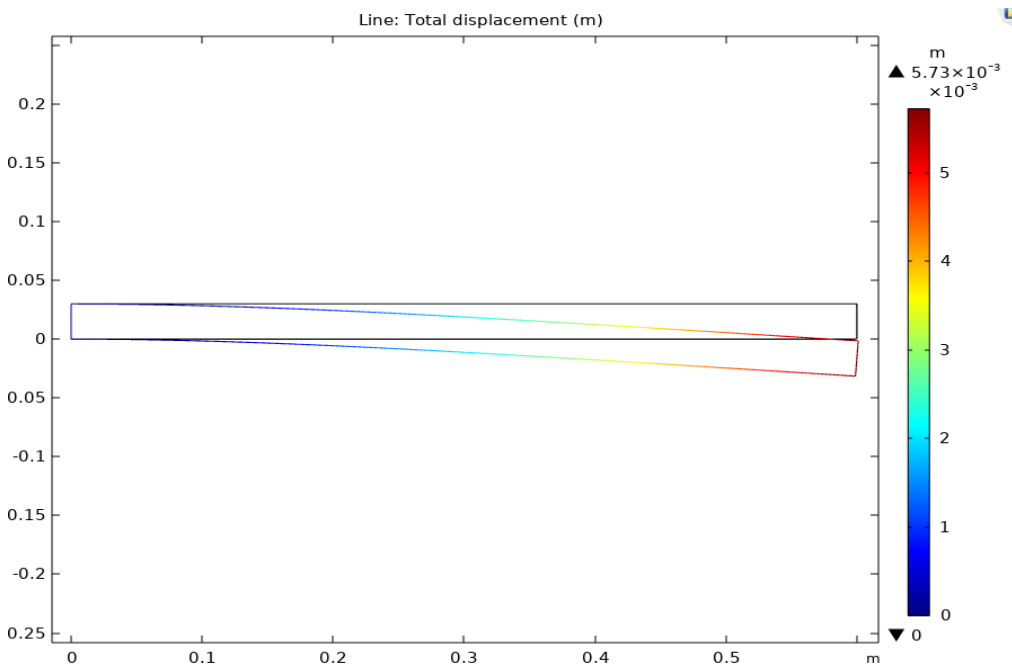
*Figure **22**. Displacement of rectangular beam under solid mechanics computation, gao jie, accessed 19/03/2020.*

Observation of how principal stress displays at cross section, which clearly reveals how stress is transforming along the chosen surface. In the diagram below, relevant principal stress at the cross section of the beam indicates different effects using solid mechanics.
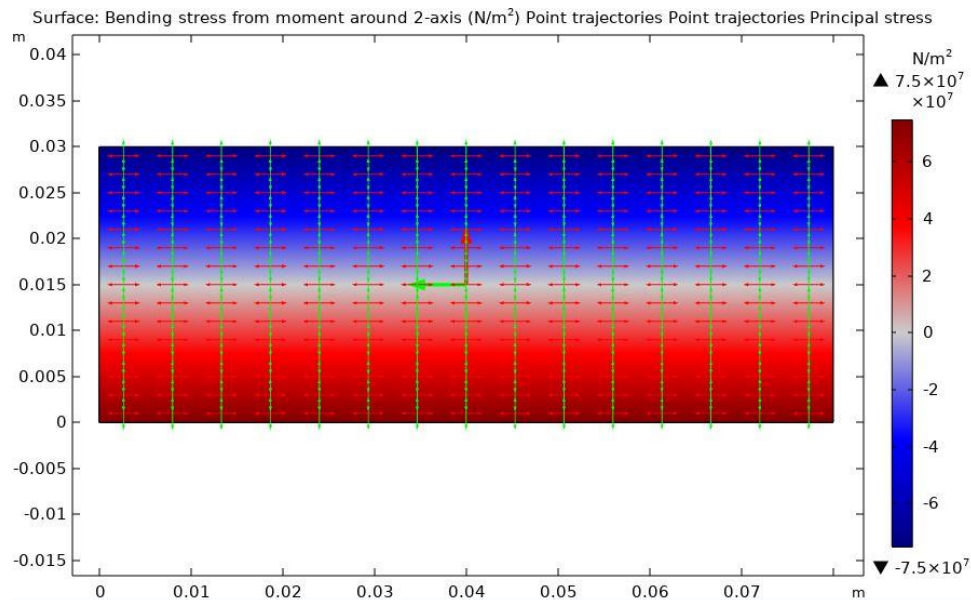
Figure 23. Stress distribution at cross section of rectangular beam by bending moment, gao jie, accessed 20/03/2020.

Afterwards, it is identical to compare results which are obtained from the counterpart study. Under beam modulus, beam formulation is detected in Comsol before commencing the computation for later contrast. To illustrate, initially, it is defined to use Euler-Bernoulli Theory (**Figure 24**).

Figure 24. Formulation of Euler-Bernoulli is used for analysis, gao jie, 19/03/2020.

49

Rather than creating a 3D object analysed beneath under solid mechanics, the object can be built in segment by vectors in the occasion of using beam modulus. Based on the concept of length-to-span ratios, the beam can be defined to be a single line segment representing the path of a beam with the cross-sectional moment of inertia. This method provides more precise critical stress magnitude once the ratio reaches certain value below 8:1.

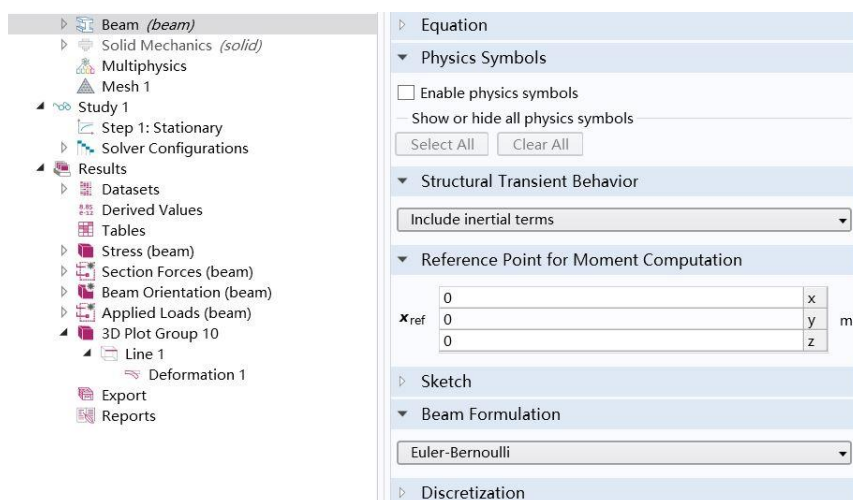To demonstrate, rectangular, square and I-beam are tested by applying bending on the entity to inspect if the result is collected with smaller error. Procedures of related simulation are presented as follow:

Since the length of object is designed as 0.6 meters, vectors are set as (0, 0.6) in length direction whereas, default values are exerted for other two directions in window of coordinate (**Figure 25**).
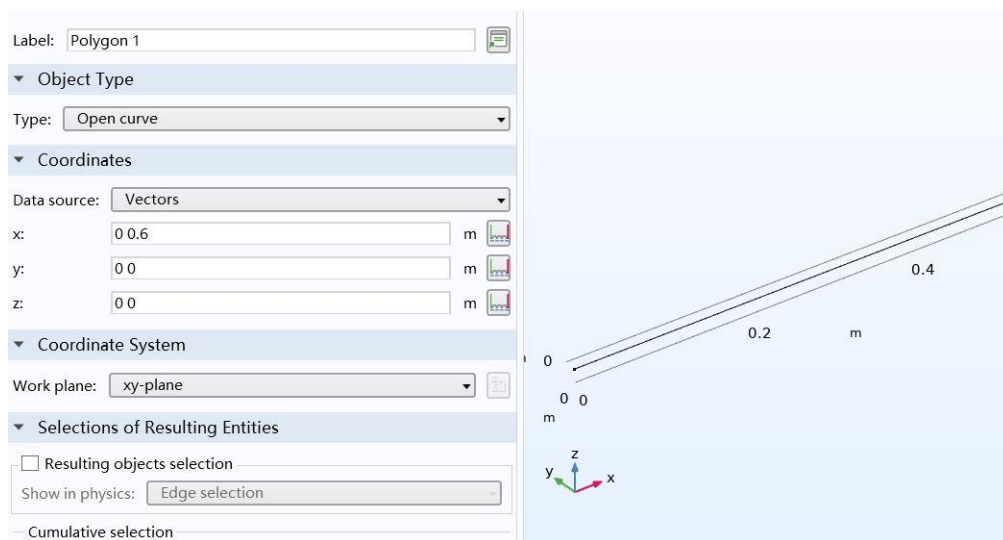
Figure 25. Build a line segment by vectors, gao jie, accessed 19/03/2020.

Aluminum is selected as material applied on the object. Subsequently, the shape of the transverse section with related properties can be defined in window of data definition (**Figure 26**), where numbers are inserted to imitate the segment to objective beams (rectangular, square and I-beam). In this occasion, load is applied at the vertex of segment while another one is fixed constraint, where the section is considered as a mass particle.
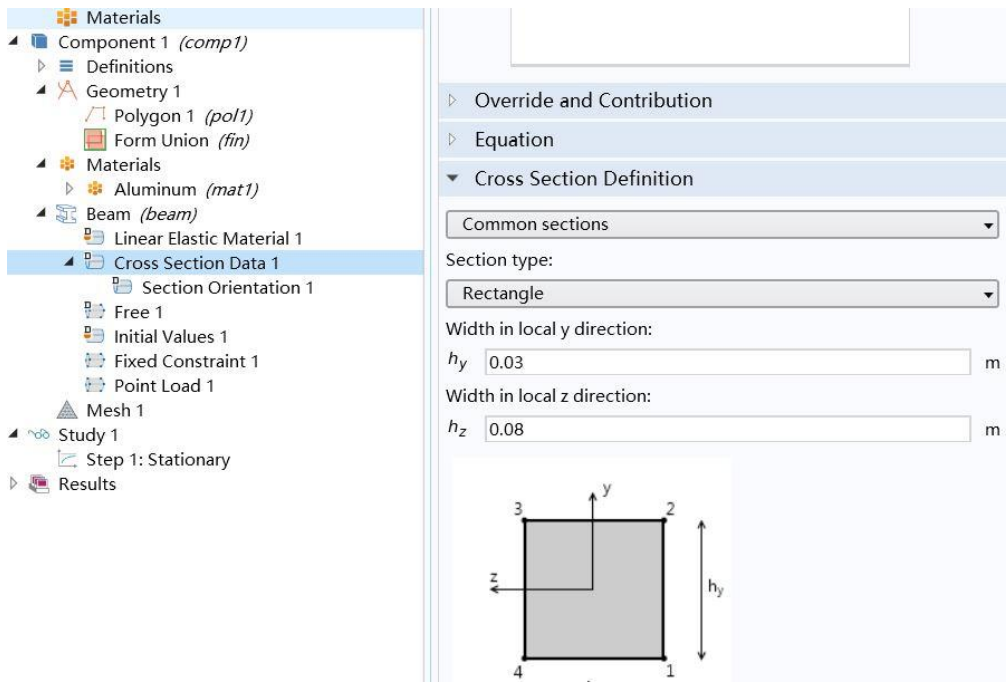
*Figure **26**. Cross section definition of rectangular beam, gao jie, accessed 19/03/2020.*

Therefore, under Euler-Bernoulli formulation, for rectangular beam:

*Figure **27**. Critical stress rectangular beam undertakes under beam modulus by bending, Euler-Bernoulli formulation, gao jie, accessed 19/03/2020.*

51

Figure 28. Displacement of rectangular beam under beam modulus by bending, Euler-Bernoulli formulation, gao jie, accessed 19/03/2020.

Where, the maximum stress undertaken is 75 MPa whereas, the maximum displacement due to mechanism is obtained as $6{,}45\ mm$.

There is one more step to swap the formulation from Euler-Bernoulli to Timoshenko in the setting window: setups are switched to Timoshenko formulation and repeat analysis. (**Figure 29**). Different result of deformation is observed after computation.
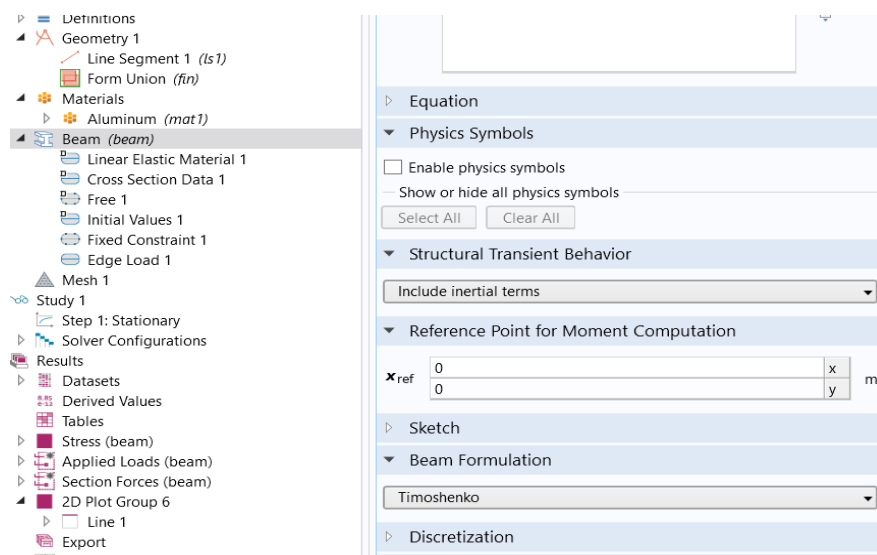
Figure 29. Timoshenko formulation is used for study, gao jie, accessed 20/03/2020.

When it uses Timoshenko formulation:
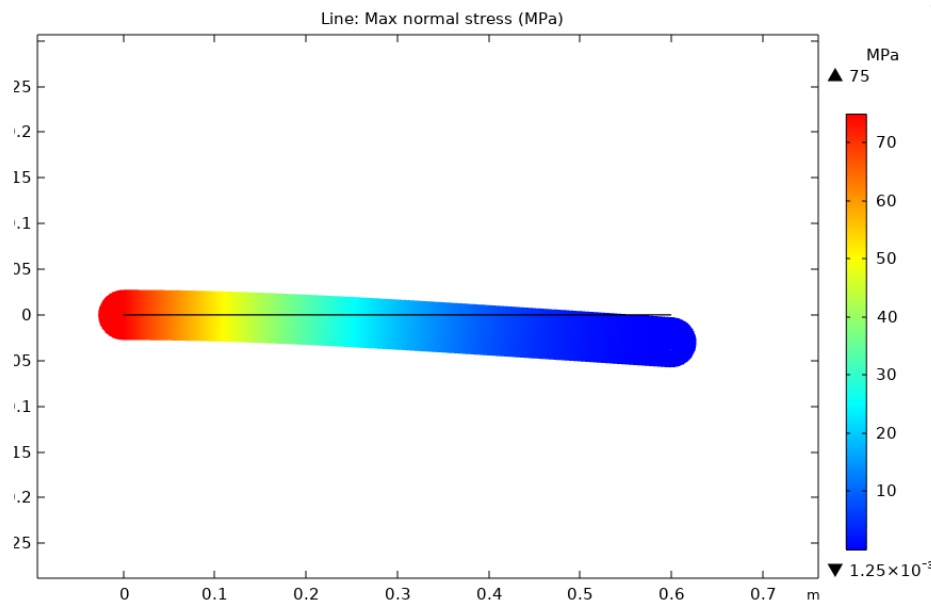
*Figure **30**. Critical stress of rectangular beam under beam modulus by bending, Timoshenko formulation, gao jie, accessed 19/03/2020.*
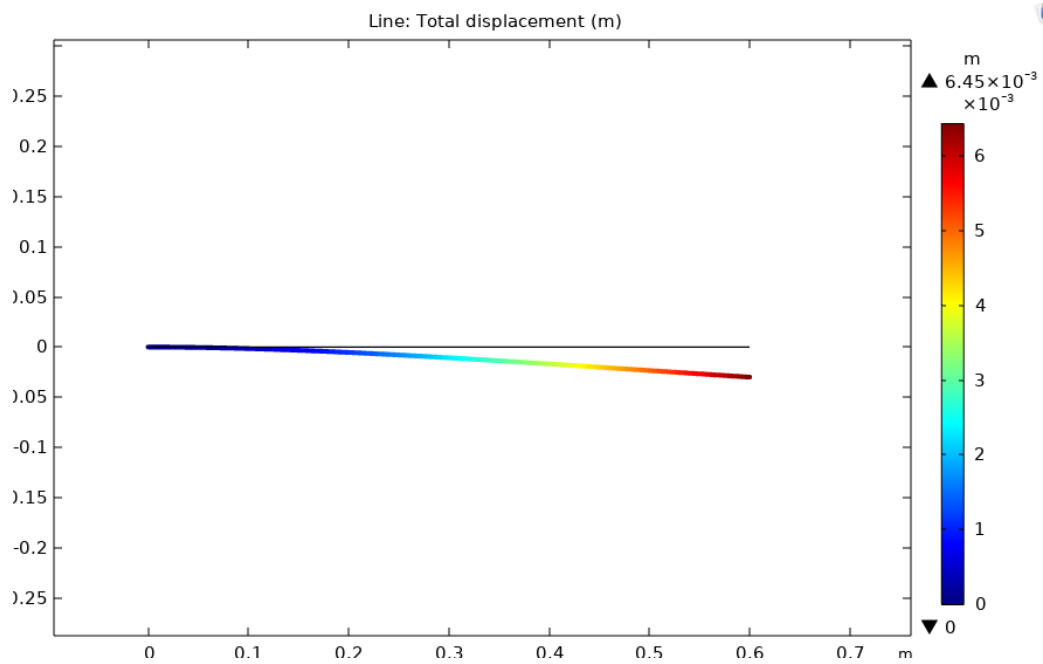
*Figure **31**. Displacement of rectangular beam under beam modulus by bending, Timoshenko formulation, gao jie, accessed 19/03/2020.*

53

Square beam:

Solid mechanics:

*Figure **32**. Critical stress and displacement of square beam by bending under solid mechanics, gao jie, accessed 20/03/2020.*

Beam modulus (by applying Bernoulli formulation):

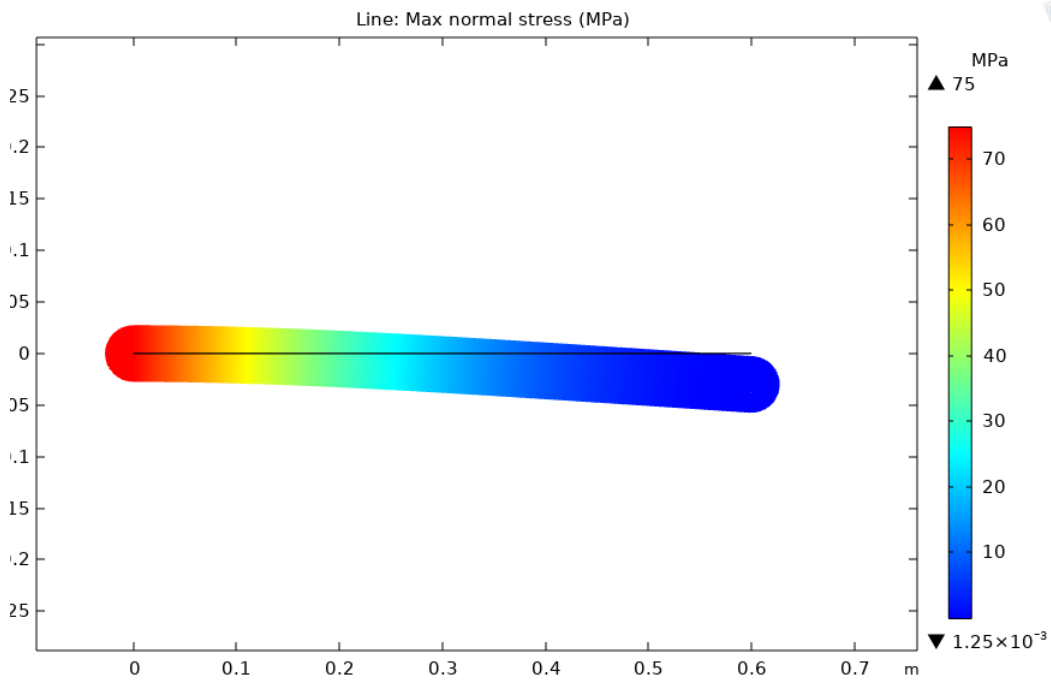*Figure 33. Critical stress square beam undertakes under beam modulus by bending, Euler-Bernoulli formulation, gao jie, accessed 19/03/2020.*
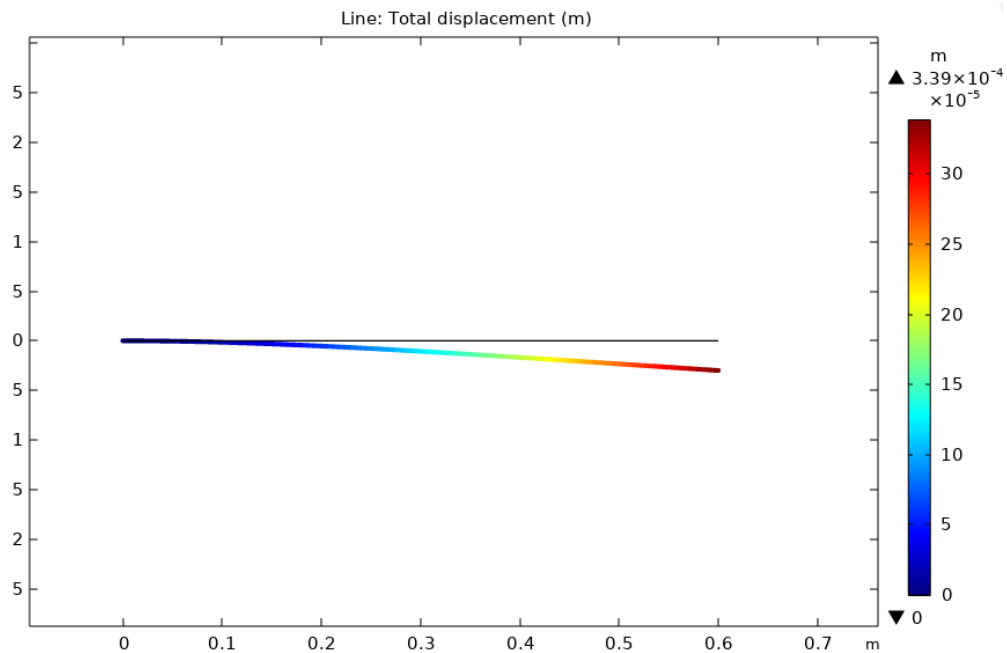
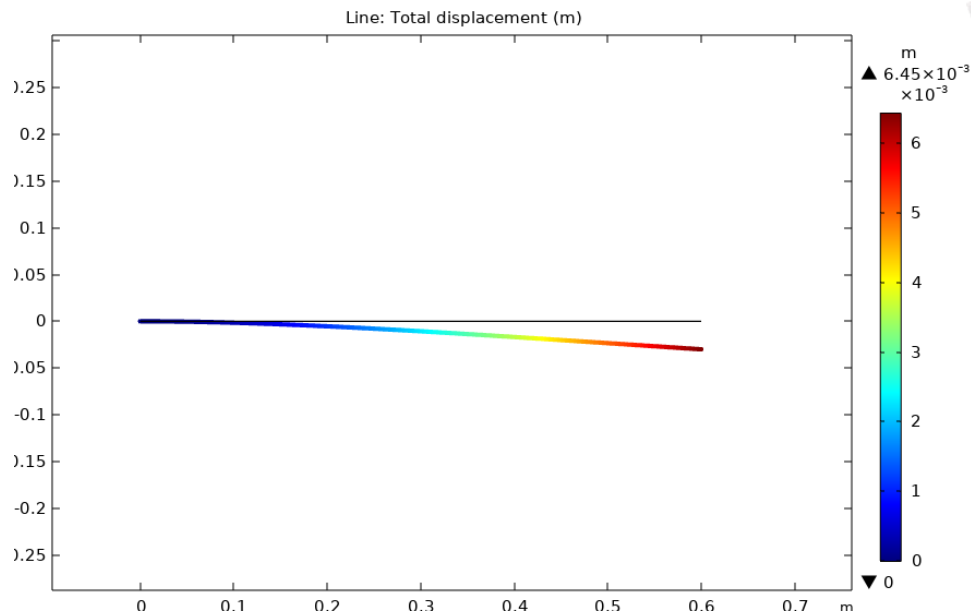*Figure 34. Displacement of square beam under beam modulus by bending, Euler-Bernoulli formulation, gao jie, accessed 19/03/2020.*

The maximum stress is obtained as 10.5 MPa and the displacement reaches a critical number of $3.39 \times 10^{-4}\ m$

Turn to Timoshenko formulation, the maximum normal stress remains still whereas, the critical displacement becomes larger:
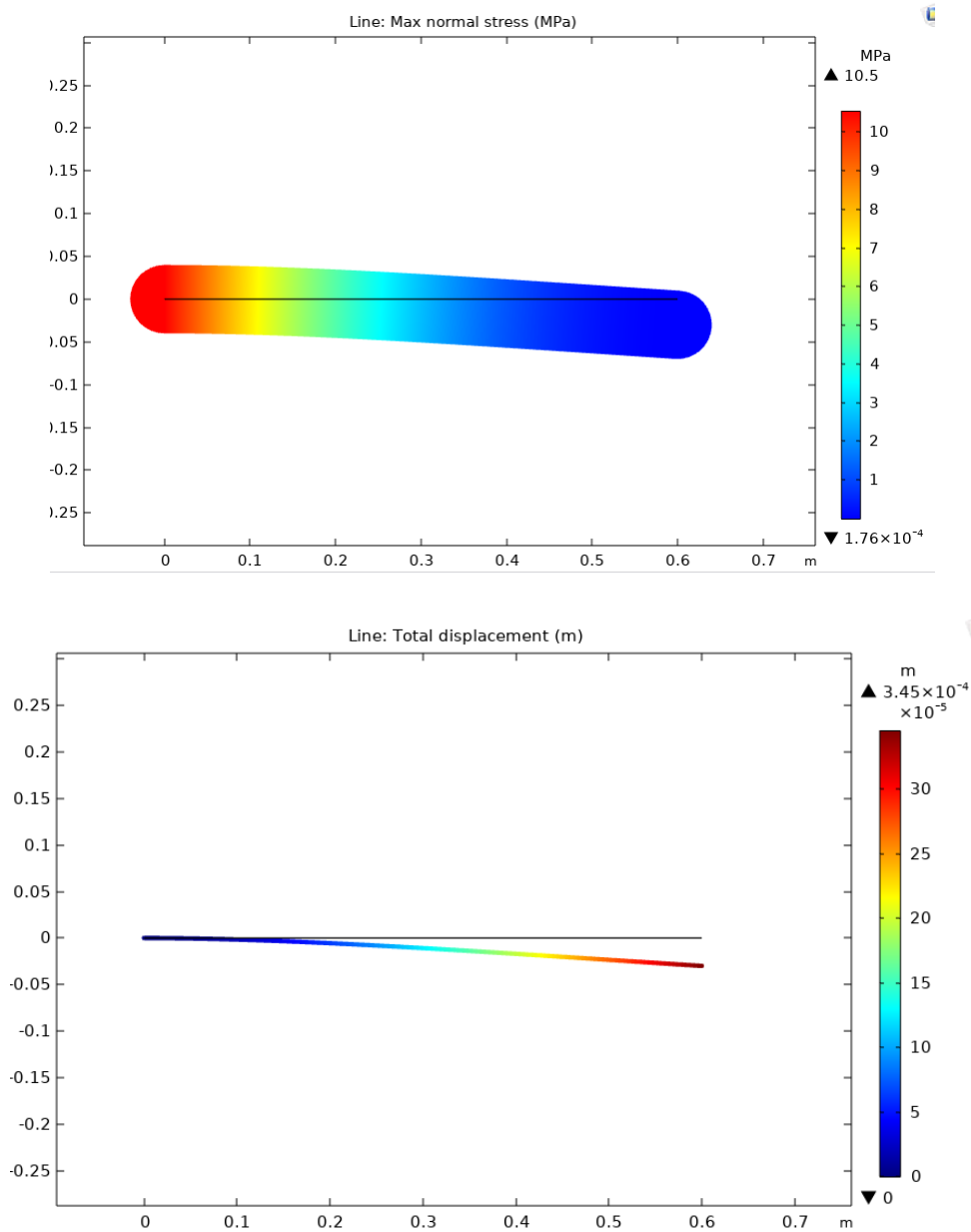
Figure 35. Critical stress and displacement of square beam under beam modulus by bending, Timoshenko formulation, gao jie, accessed 19/03/2020.

The maximum stress is obtained as 10.5 MPa and the displacement reaches a critical number of $3.45 \times 10^{-4}\ m$

Thin I-beam (thickness of 0.03 m):

To make the results more convincible, I-beams are inspected in addition for proof of disparities. Under solid mechanics:
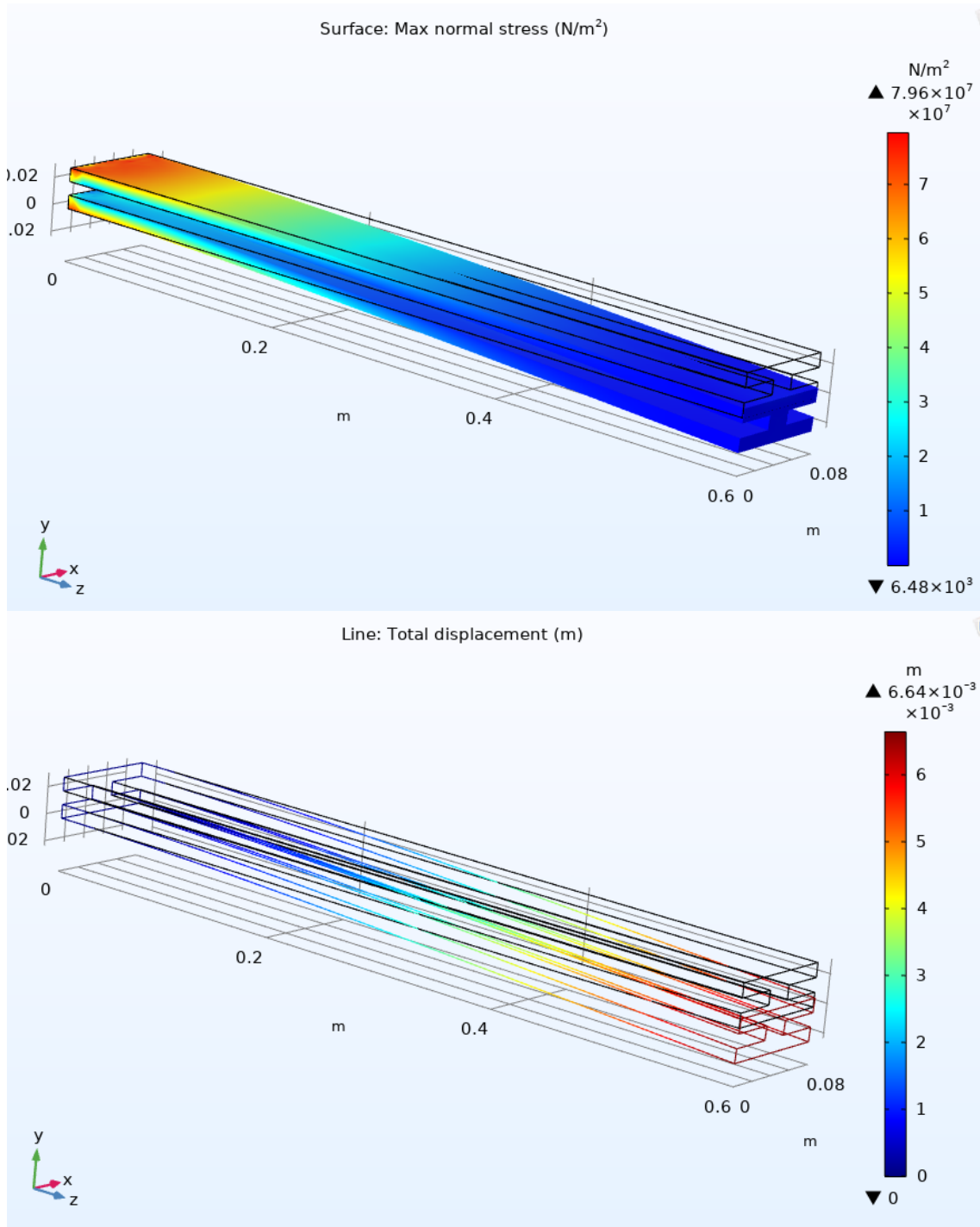
Figure 36. Critical stress and displacement of thin I-beam by bending under solid mechanics, gao jie, accessed 20/03/2020.

Beam modulus: modify the cross-section definition with H-shape beams and insert the designed dimensions before embarking with the computation.
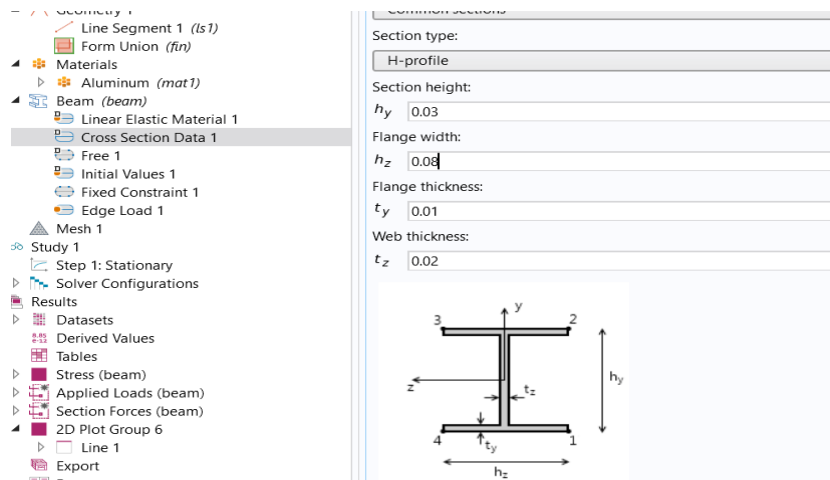
Figure 37. Cross section definition of thin I-beam, gao jie, accessed 19/03/2020.

By using Euler-Bernoulli formulation:
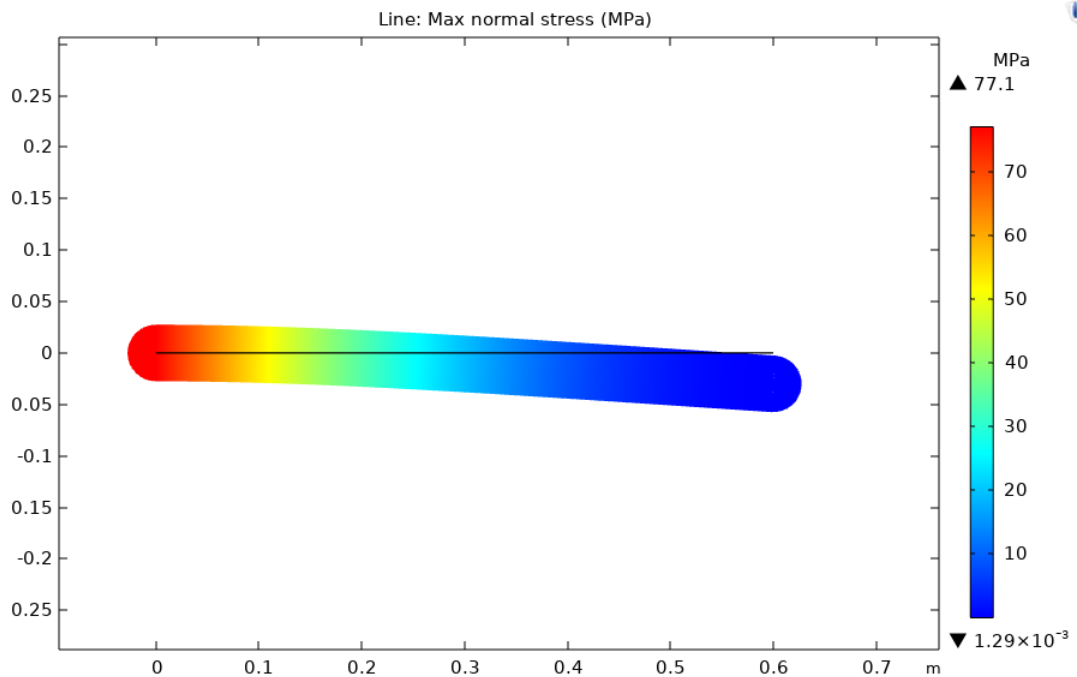
Figure 38. Critical stress undertaken of thin I-beam under beam modulus by bending, Euler-Bernoulli formulation, gao jie, accessed 19/03/2020.
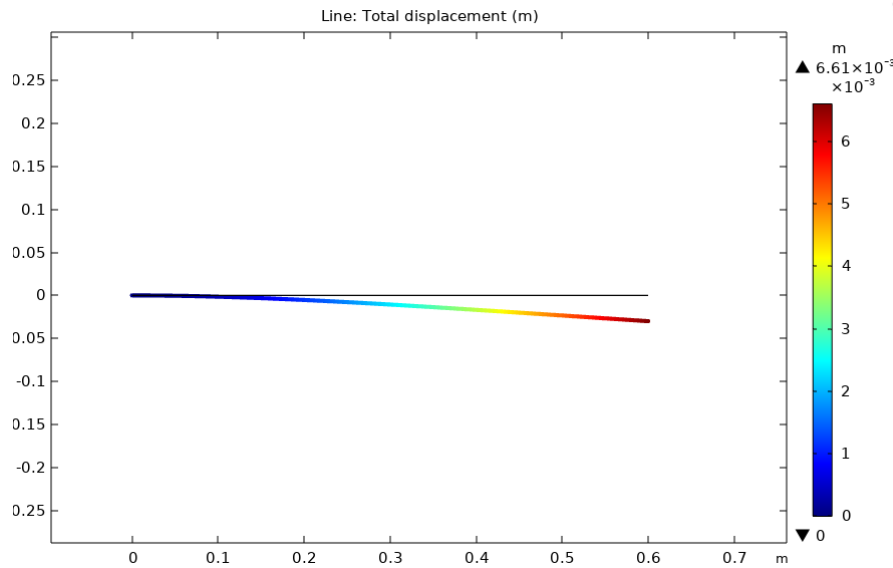
*Figure **39**. Displacement of thin I-beam under beam modulus by bending, Euler-Bernoulli formulation, gao jie, accessed 19/03/2020.*

By using Timoshenko formulation, results remain still: the maximum normal stress is collected as 77.1 MPa and displacement reaches 6.61 mm for critical.

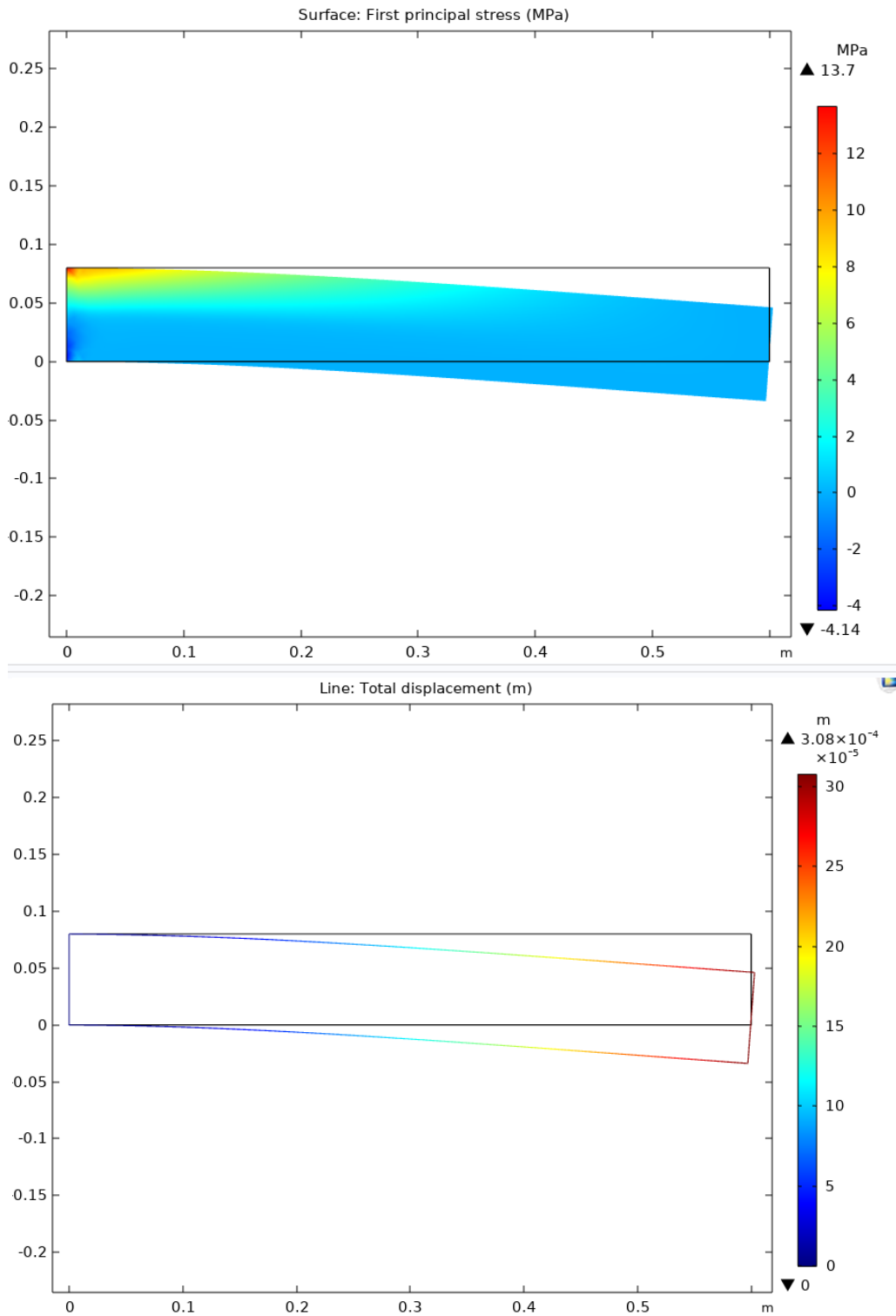**Thick I-beam (thickness of 0.08 m):**

Solid mechanics:
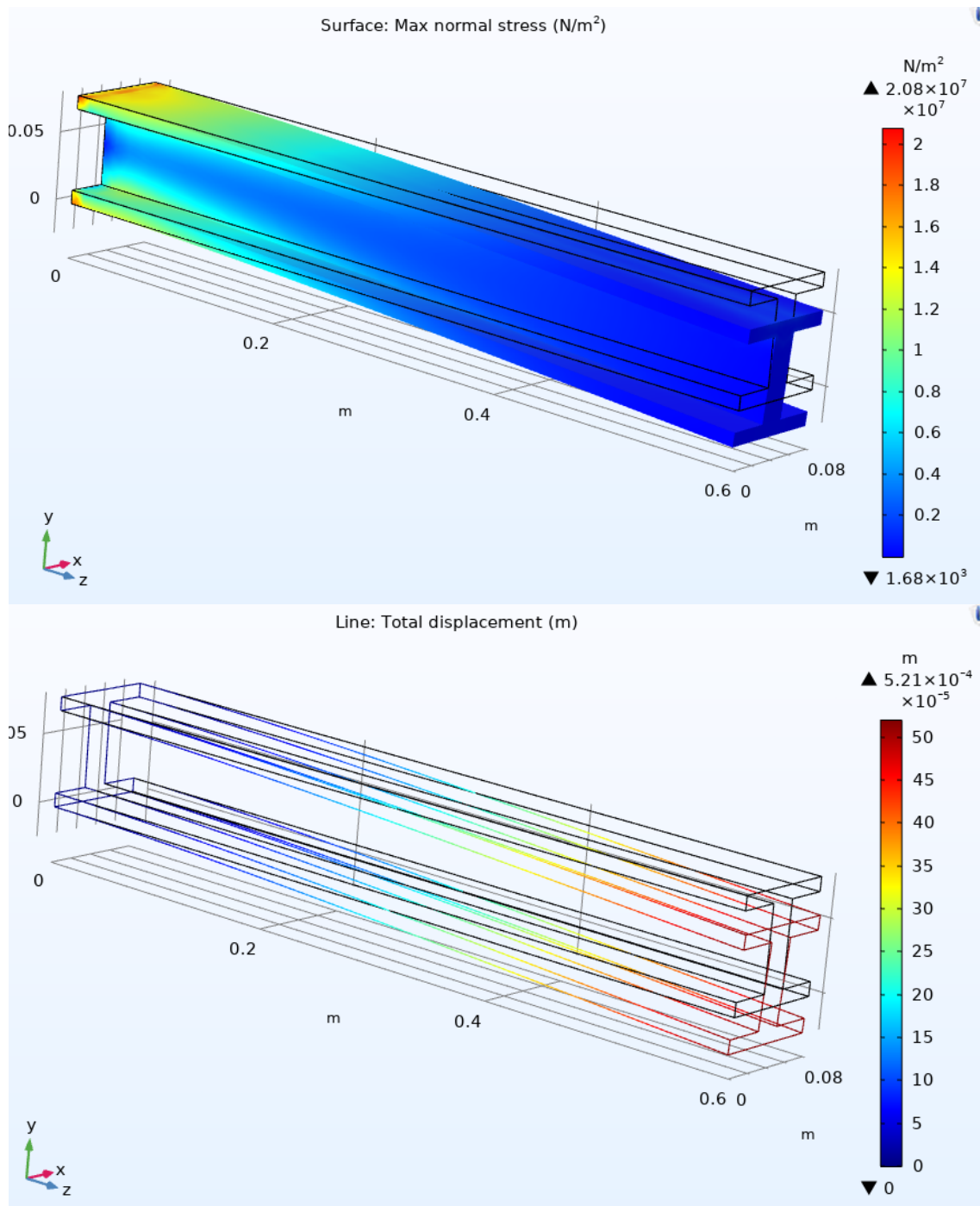
*Figure **40**. Critical stress and displacement of thick I-beam by bending under solid mechanics, gao jie, accessed 20/03/2020.*
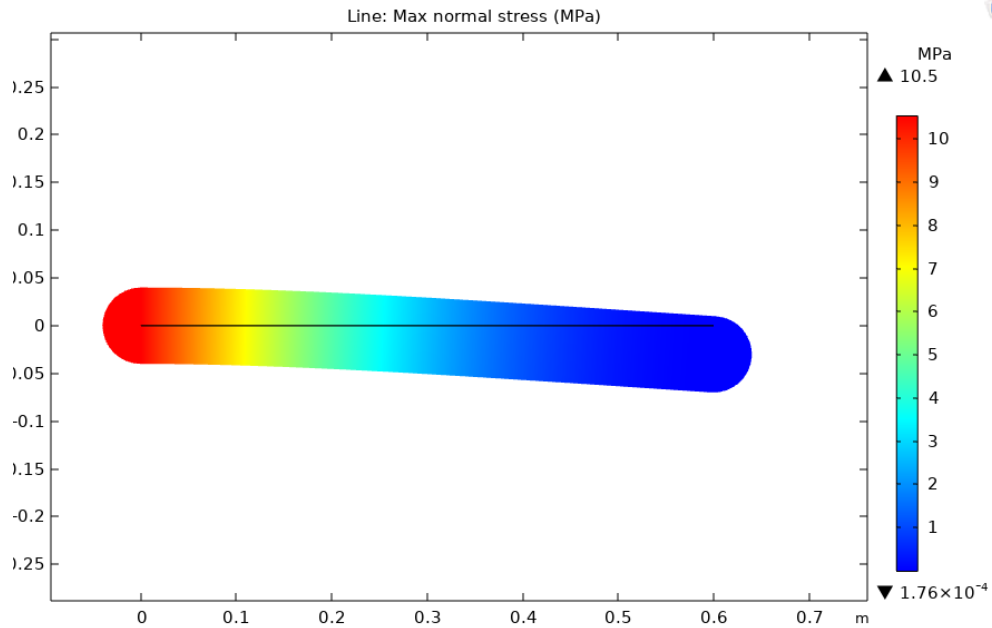
Beam modulus (by using Bernoulli formulation):
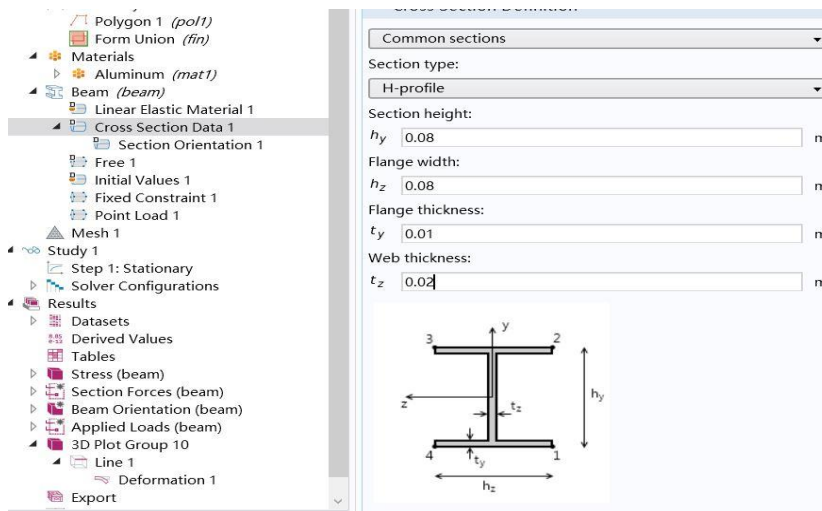
*Figure **41**. Cross section definition of thick I-beam, gao jie, accessed 19/03/2020.*
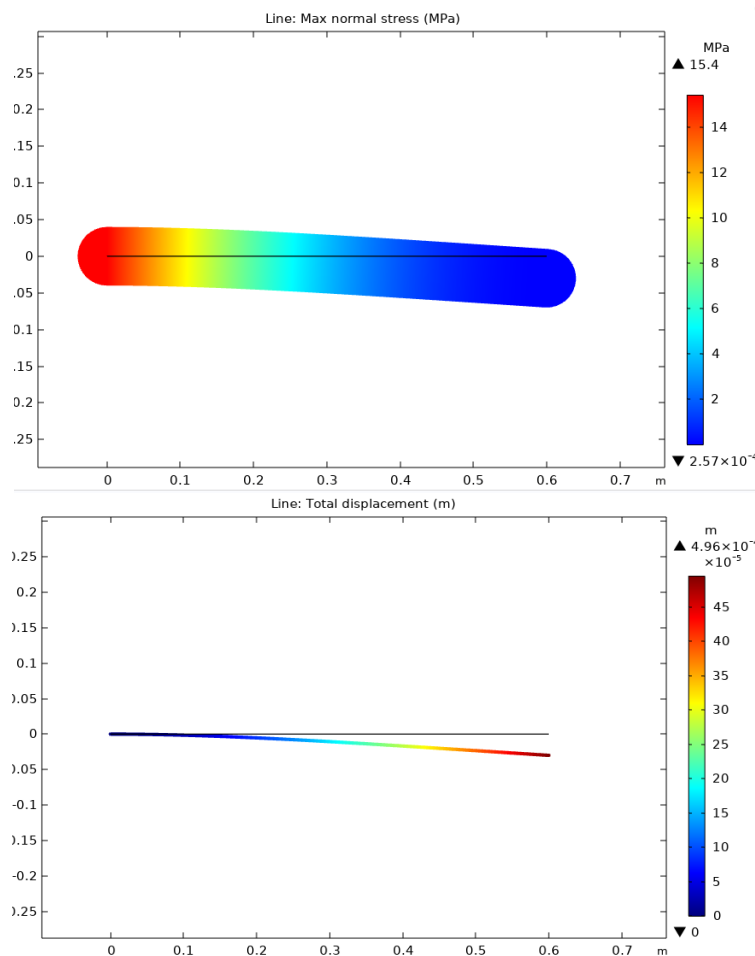
*Figure **42**. Critical stress undertaken and displacement of thick I-beam under beam modulus by bending, Euler-Bernoulli formulation, gao jie, accessed 17/04/2020.*

61

Switch to Timoshenko formulation, result is collected as:
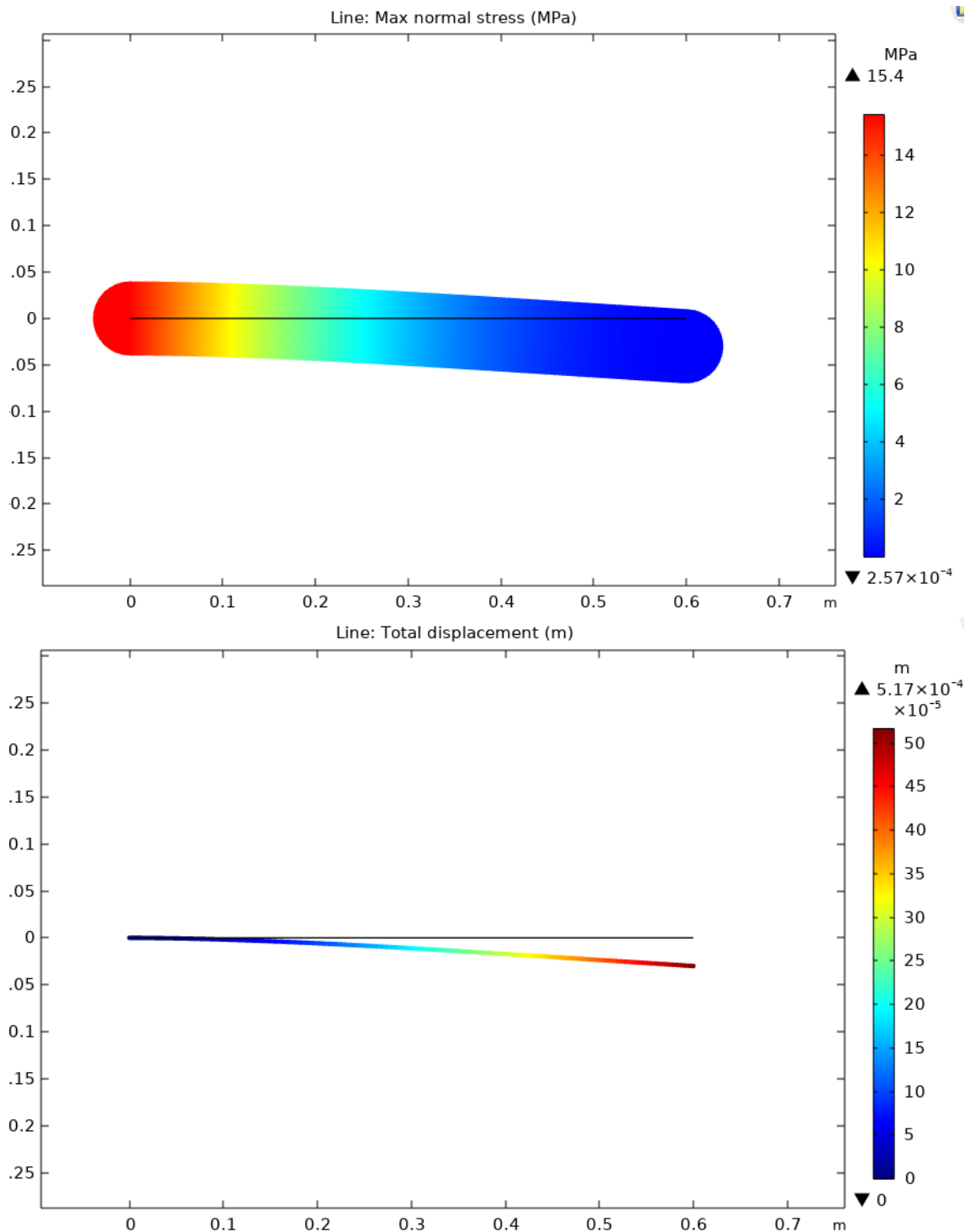
*Figure **43**. Critical stress and displacement of thick I-beam by bending under beam modulus, Timoshenko formulation, gao jie, accessed 20/03/2020.*

To summarize analytical results of beams under surface load case:

Table 10. Results of surface load occasion.

Surface load	Rectangular (0,08m*0,03m)	Square (0,08m*0,08m)	I-beam (0,03m thick)	I-beam (0,08m thick)
Mathematical calculation				
Maximum normal stress (MPa)	75	10,55	77,14	15,4
Maximum displacement (mm)	6,45	0,339	6,61	0,495
Solid mechanics				
Maximum normal stress (MPa)	79	13,7	79,6	20,8
Maximum displacement (mm)	5,75	0,308	6,64	0,521
Euler-Bernoulli formulation				
Maximum normal stress (MPa)	75	10,5	77,1	15,4
Maximum displacement (mm)	6,45	0,339	6,61	0,496
Timoshenko formulation				
Maximum normal stress (MPa)	75	10,5	77,1	15,4
Maximum displacement (mm)	6,45	0,345	6,61	0,517

4.2.2 Axial load simulation

Likewise, make analogous experiments and compare results from two different analysis moduli. Axial load is defined as 1000 N which is applied vertical to transverse section of beams. To illustrate, **Rectangular beam** under solid mechanics analysis:
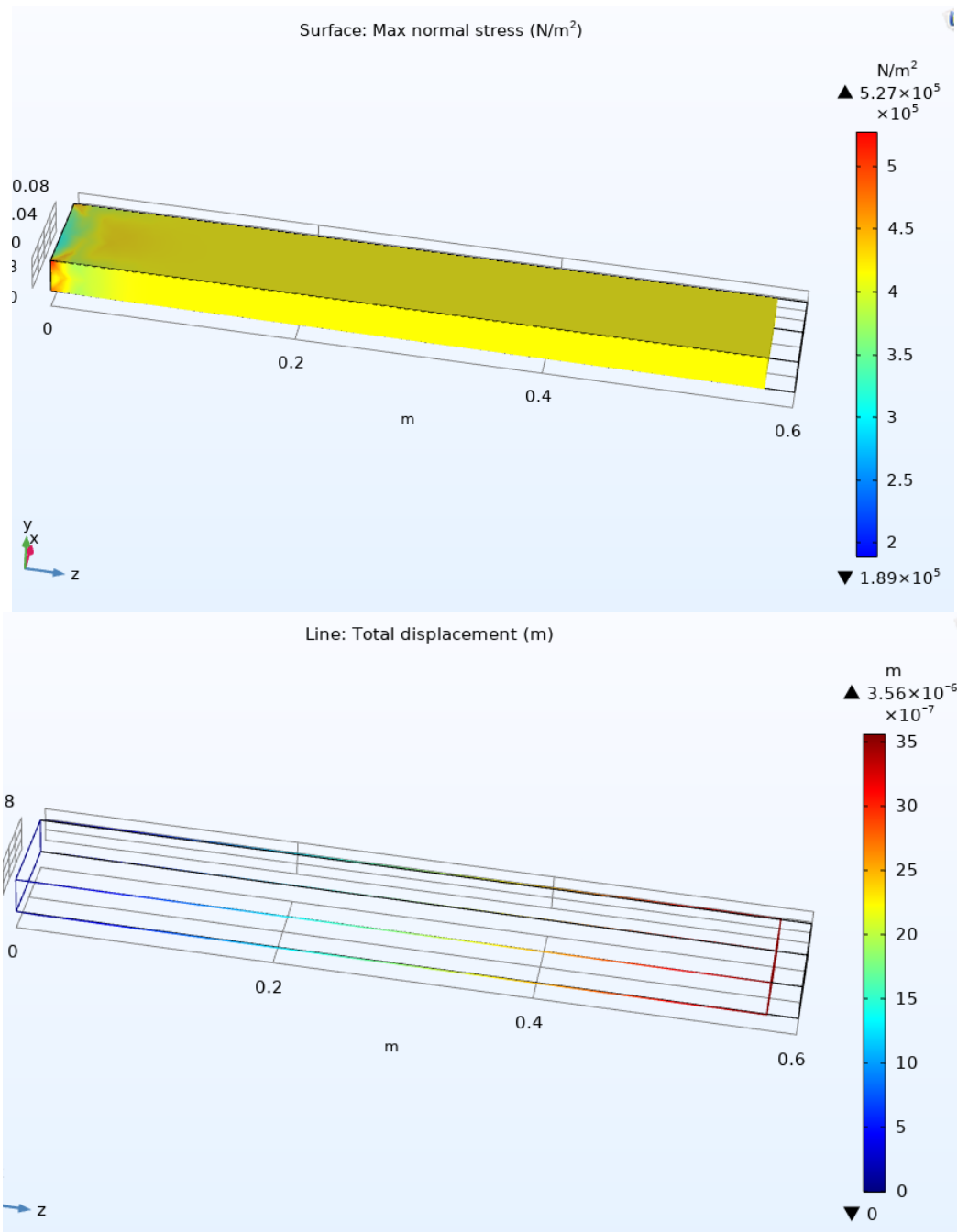
*Figure **44**. Critical stress and displacement of rectangular beam under solid mechanics analysis by axial load, gao jie, accessed 20/03/2020.*

Under beam modulus: by Euler-Bernoulli formulation when axial load is applied:
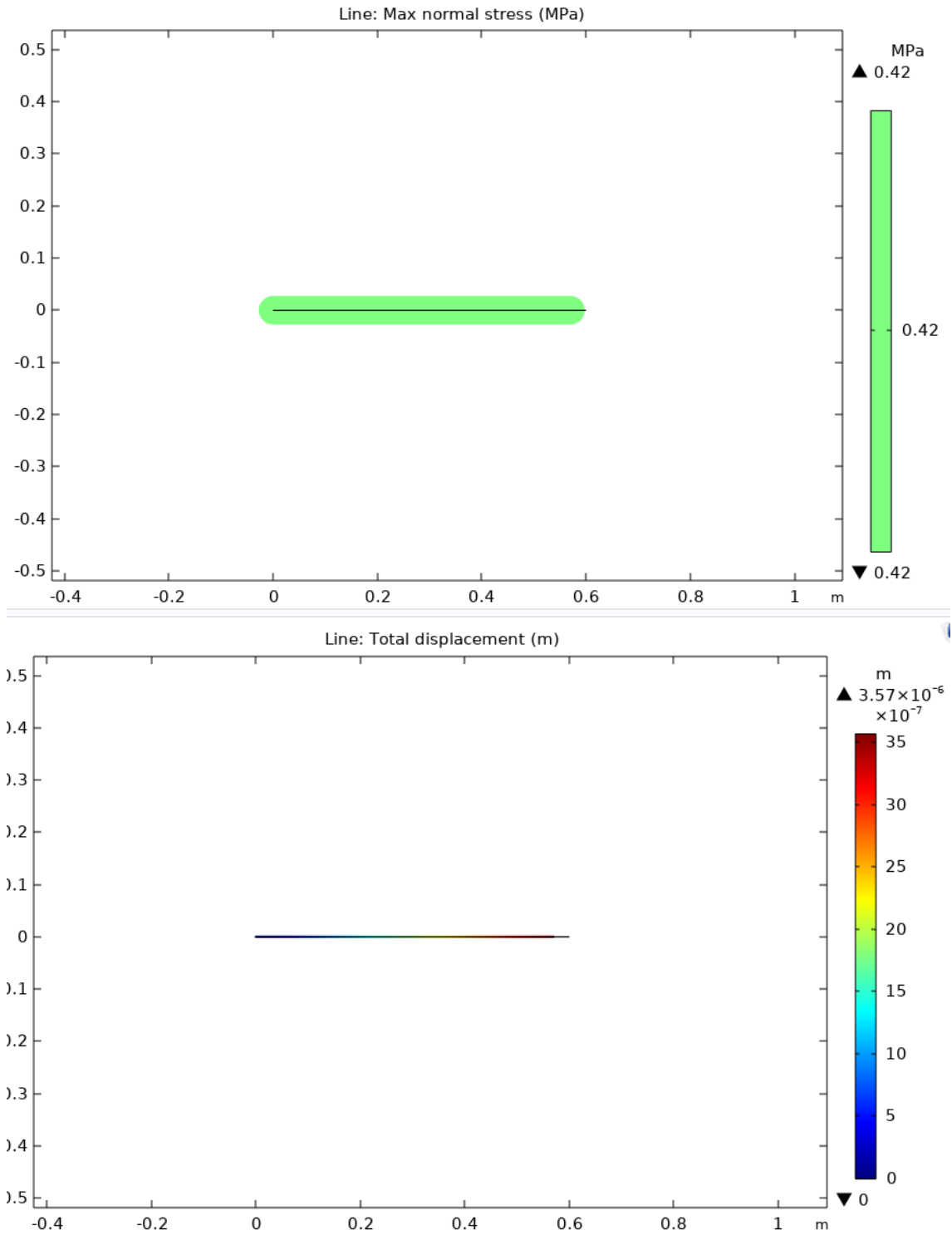
*Figure **45**. Critical stress and displacement of rectangular beam by Bernoulli formulation under beam modulus by axial load, gao jie, accessed 20/03/2020.*

By Timoshenko formulation:
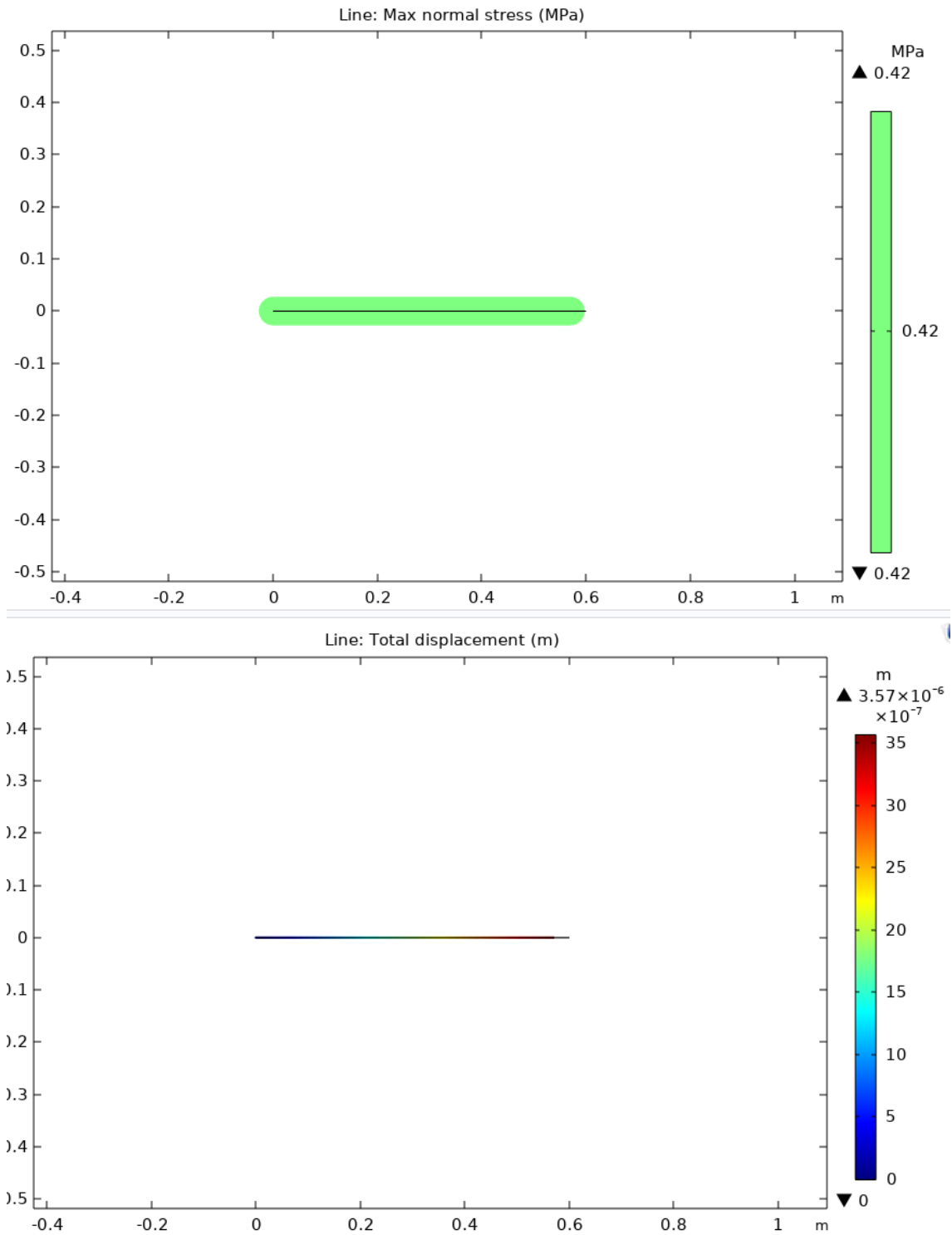
Figure 46. Critical stress and displacement of rectangular beam by Timoshenko formulation under beam modulus by axial load, gao jie, accessed 20/03/2020.

No difference is captured between results when formulation is switched.

Square beam:

Under solid mechanics:
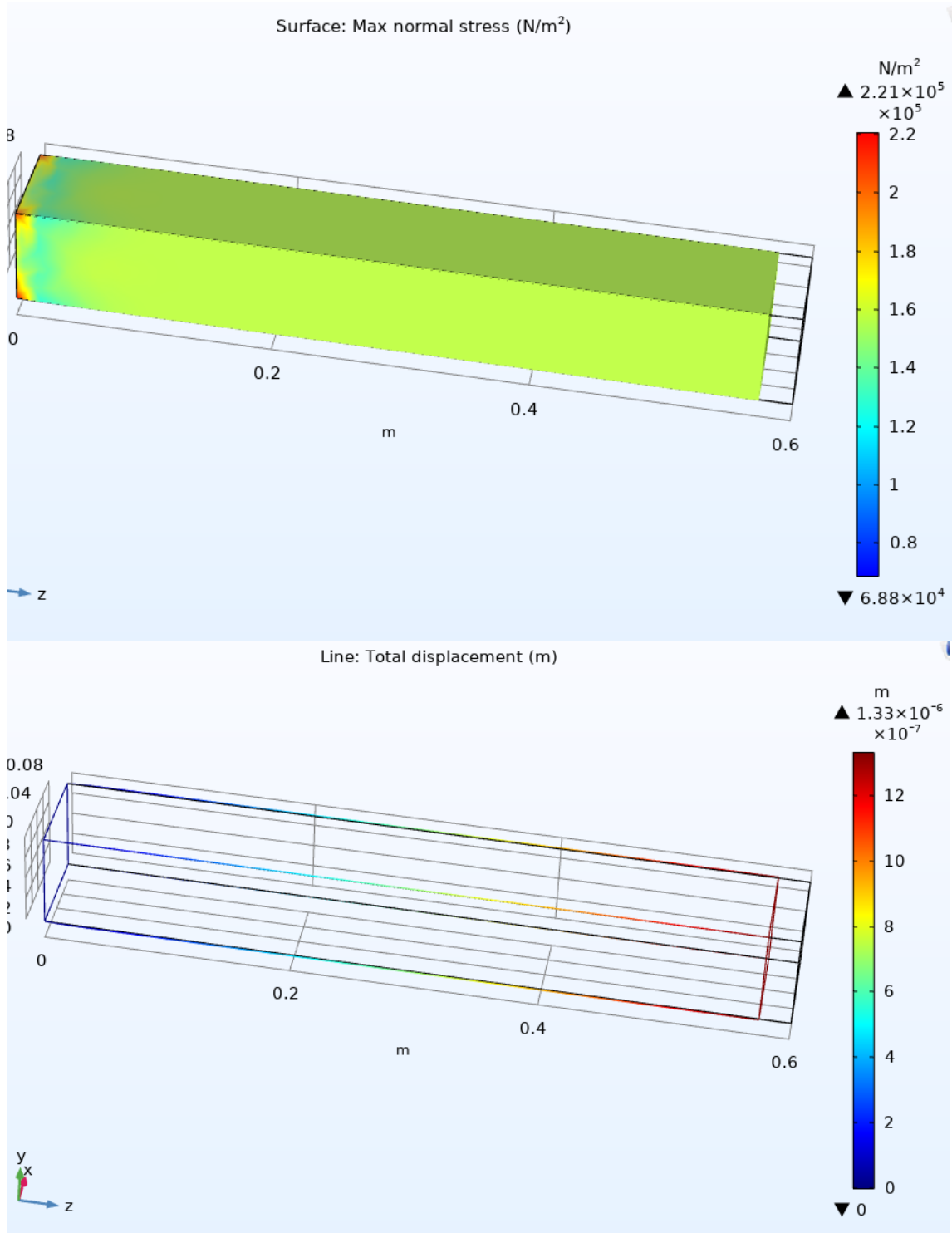
*Figure **47**. Critical stress and displacement of square beam under solid mechanics analysis by axial load, gao jie, accessed 20/03/2020.*

Under beam modulus: (for both Euler-Bernoulli and Timoshenko formulation)
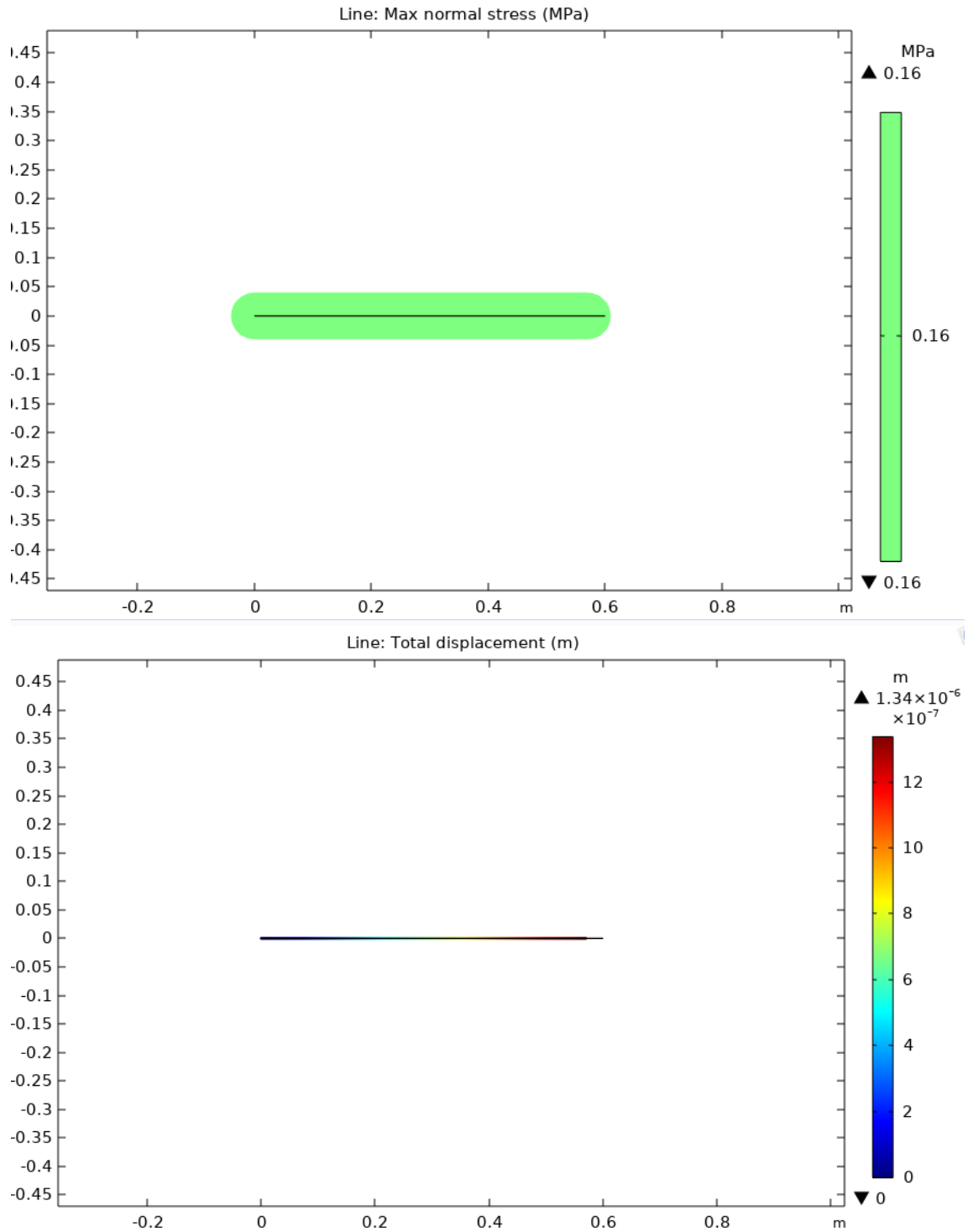
Figure 48. Critical stress and displacement of square beam by both Euler-Bernoulli and Timoshenko formulation under beam modulus by axial load, gao jie, accessed 20/03/2020.

Hence, to summarize, results which are collected from analysis of beams with different under various moduli are shown in table below:

Table 11. Results of axial load occasion.

Axial load	Rectangular (0,08m*0,03m)	Square (0,08m*0,08m)	I-beam (0,03m thick)	I-beam (0,08m thick)
Mathematical cal- culation				
Maximum normal stress (MPa)	0,42	0,16	0,56	0,36
Maximum dis- placement (mm)	3,57E-03	1,34E-03	4,78E-03	3,06E-03
Solid mechanics				
Maximum normal stress (MPa)	0,527	0,221	0,744	0,532
Maximum dis- placement (mm)	3,56E-03	1,33E-03	4,75E-03	3,05E-03
Euler-Bernoulli formulation				
Maximum normal stress (MPa)	0,42	0,16	0,56	0,36
Maximum dis- placement (mm)	3,57E-03	1,34E-03	4,76E-03	3,06E-03
Timoshenko formu- lation				
Maximum normal stress (MPa)	0,42	0,16	0,56	0,36
Maximum dis- placement (mm)	3,57E-03	1,34E-03	4,76E-03	3,06E-03

4.2.3 Torsion simulation

A torque of $500 \, N \cdot m$ is induced on objective beams to simulations. Results are aggregated in the table below which contains related numbers showing critical stress as well as displacement. Data which is collected from various moduli are shown in table below:

Table 12. Results of torsion occasion.

Torsion	Rectangular (0,08m*0,03m)	Square (0,08m*0,08m)	I-beam (0,03m thick)	I-beam (0,08m thick)
Mathematical calculation				
Maximum normal stress (MPa)	26,7	4,7	72,14	15,4
Twist angle (rad)	0,021	1,98E-03	0,661	3,07E-03
Solid mechanics				
Maximum normal stress (MPa)	29,4	5,41	74,4	16,9
Twist angle (rad)	2,80E-02	2,03E-03	4,75E-03	3,15E-03
Euler-Bernoulli formulation				
Maximum normal stress (MPa)	26,6	4,7	72,1	15,4
Twist angle (rad)	0,021	1,98E-03	0,661	3,08E-03
Timoshenko formulation				
Maximum normal stress (MPa)	26,7	4,7	72,1	15,4
Twist angle (rad)	0,021	1,99E-03	0,662	3,11E-03

5. DISCUSSIONS

There are 24 simulation occasions presented in total which are experimented to demonstrate discrepancies between Euler-Bernoulli Beam Theory and Timoshenko Beam Theory while applying to beam elements. Additionally, differences between solid mechanics analysis and beam modulus as well are compared in pairs. Each shape of beams is modelled under solid mechanics and beam modulus where two formulations are exerted in sequence. Further, both stress and displacement of the beam are collected after that simulations are complete. Results which contain the maximum stress and displacement of the beam by bending conducted by distributed surface load using solid mechanics as well as comparison of exerting Euler-Bernoulli and Timoshenko formulation under beam modulus are summarized in tables (**Table 10**) from the last section**.**

Likewise, results from other occasions are compared and inscribed in tables which are presented in the former section (**Table 11&12**), where stress and displacement (twisted angle) of beams with different shapes of cross section by axial load and torsion as well using solid mechanics and beam modulus are involved (listed below for convenience of inspection).

In conclusion, by using beam modulus for analysis, to a large degree, results are acquired more accurate when compared with the mathematical calculations on both critical values of stress and displacement than ones from solid mechanics. This is due to disparities on degrees of freedom where solid mechanics includes three directions heading to axes which leads to a higher error during computation. Since beam modulus allows all six degrees of freedom which means in rotary directions where motions are included which produces more precise data. The stress is aggregated around the fixed end and becomes loose at the free end. In vertical direction, stress is higher at the surface and decouples symmetrically when it approaches to the neutral axis. The maximum stress is obtained at the corner of the beam at the fixed end from the computation results. This result is conducted since when a shear load is applied at the free

71

end, a moment arm which is the right distance from the force to the fixed boundary produces the bending moment, after which there will be a deformation. By investigating plot of principal stress, stress is disseminating from the location where it is applied to the fixed end. Moreover, since the resistance at the surface level at the fixed constraint boundary is larger to be counter, which makes the region more difficult to stretch, the stress hence becomes denser than the area near the neutral axis.

Another distinction which is visible after study is that for **a beam object with a certain length**, when beams are encountering a uniform distributed surface load, which induces a bending moment further, thin beams (square beams and I-beam with thickness of 0.03 metres) simulated under beam modulus with Euler-Bernoulli formulation perform same maximum stress and displacement as when beams are analysed under Timoshenko formulation (**Table 10**). In contrast, thick beams provide differences on the magnitudes of maximum displacement when there is a replacement of formulation during the study. Timoshenko formulation produces a larger critical displacement of the beam than Euler-Bernoulli formulation. An analogous finding is spectated under torsion occasion when Timoshenko formulation is applied, thick beams offer twisted angle with a higher number than Euler-Bernoulli formulation. Nevertheless, situations appear different when axial load is applied in use. To investigate the other simulation results, beams which are studied under axial load disobey the regulation captured by contrast of that in bending occasion since axial load do not produce shear deformation.

Hence, it is concluded that when **objects of a still length** are under study for both bending and torsion cases, if the thickness of beams increases, Timoshenko Theory can result more precise on deformation (larger displacement at free end) than Euler-Bernoulli Theory. Since a rotation which is derived from a shear deformation, not included in a Bernoulli Theory, displays under Timoshenko formulation. Furthermore, another parameter which may affect the final findings is the length of the beam. Referring to the concept mentioned in literature review, length-to-thickness ratio somehow will influence precision of results.

Hereby, how precise the results are will depend on the length-to-thickness ratio rather than only relying on thickness of the beam.

However, experiments still involve flaws. There ought to be a fundamental difference visible to readers. For Euler-Bernoulli Beams, the free end stays perpendicular to the neutral axis after bending while Timoshenko Beams offer an acute angle. This is not captured within simulations above. It is due to relation between length and thickness which is considerably large that gives technical errors. For Timoshenko Beams, the length should be designed shorter (which induces to a higher eigenfrequency).

6. CONCLUSIONS

The main orientation of the thesis is to present and compare the discrepancy between two delegative beam theories which are prevalently applied in both civil engineering and structural analysis. The objectives of the thesis are eventually achieved via Comsol computation and by observing the stress distribution along the entity of beam elements and deformation after importing either a force or moment to the domain. Beams with different thickness as well as different shapes are used to make contrast which demonstrates the differences between Euler-Bernoulli Beam Theory and Timoshenko Beam Theory.

For instructions, to anyone who is newly involved to this related project, a tutorial which is listed in Comsol application libraries.
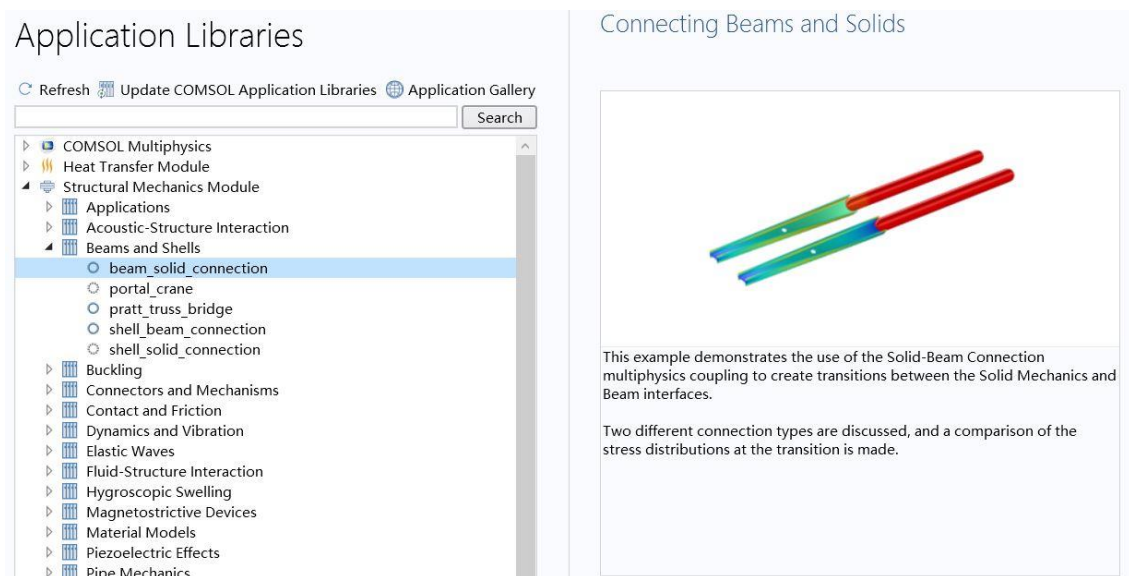
Figure 49. Tutorial read for new engineers, gao jie, accessed 20/04/2020.

In conclusion, when **objects of a still length** are under study for both bending and torsion cases, if the thickness of beams increases, Timoshenko Theory can result more precise on deformation (larger displacement at free end) than Euler-Bernoulli Theory. Since a rotation which is derived from a shear deformation, not included in a Bernoulli Theory, displays under Timoshenko formulation. Fur-

thermore, another parameter which may affect the final findings is the length of the beam. Referring to the concept mentioned in literature review, length-to-thickness ratio somehow will influence precision of results. Hereby, how precise the results are will depend on the length-to-thickness ratio rather than only relying on thickness of the beam. Moreover, by using beam modulus for analysis, to a large degree, results are acquired more accurate when compared with the mathematical calculations on both critical values of stress and displacement than ones from solid mechanics.

For further investigation, this thesis furnishes rather obscure conclusions to Euler-Bernoulli Beam Theory and its counterpart as well, since the tool used is not representative enough to publish more accurate find-outs. Methods as well as dimension of objectives are remaining flaws which failed to investigate the distinct on the angle of the end after bending. Other computation methods ought to be used such as Matlab and so forth to explore more evidence for demonstration. Meanwhile, more beams with different shapes are recommended to be input for case study.

7. REFERENCES

Simscale.com. (2019). *What is FEA | Finite Element Analysis? — SimScale Documentation*. [online] Available at:
https://www.simscale.com/docs/content/simwiki/fea/whatisfea.html.
[Accessed at 27/02/2020]

GoEngineer. (2016). *SOLIDWORKS Simulation - Comparison Between Solid and Beam Type Elements*. [online] Available at:
https://www.goengineer.com/2016/09/01/14199/blog/
[Accessed 27 Feb. 2020].

Carbon Fibre Go-Kart Torsion Bar Final Year Project. [online] Available at:
http://doddproject.blogspot.com/2014/01/torsion-of-rectangular-cross-section.html [Accessed 27 Feb. 2020].

engineeringlibrary.org. (n.d.). *Beam Torsion | Engineering Library*. [online] Available at: https://engineeringlibrary.org/reference/beam-torsion-air-force-stress-manual
[Accessed 27 Feb. 2020].

ResearchGate. (2019). *ResearchGate | Share and discover research*. [online] Available at: https://www.researchgate.net/. [Accessed 3 Mar. 2020]

Doshi, Chinubhai, "On the Analysis of the Timoshenko Beam Theory With and Without Internal Damping" (1979). Thesis. Rochester Institute of Technology. [Accessed 19/02/2020]

Ellobody, E., Feng, R. & Young, B. (2013). *Finite Element Analysis and Design of Metal Structures*. Butterworth-Heinemann.

Gere, J. M. & Timoshenko, S. P. (1997). *Mechanics of materials*. 3.ed. London: Chapman & Hall.

Hibbeler, R.C. & Kai Beng Yap (2018). *Mechanics of materials*. Harlow Pearson. Tenth Edition, p22-45, p97-165, p201-384, p463-499, p595-599, p629-631.

Hughes, A.F., Iles, D.C., Malik, A.S. and Steel Construction Institute (Great Britain (2011). *Design of steel beams in torsion*: in accordance with Eurocodes and UK national annexes. Ascot: Sci.

Megson, T. H. G. & Megson, T. H. G. (2005). *Structural and Stress Analysis.* Burlington: Butterworth-Heinemann.

O.A. Bauchau & J.I. Craig (2009). *Structural Analysis with application to aerospace structures*. 1st Edition, Springer Science & Business Media, Heidelberg, Germany.

Protter, Murray H.; Morrey, Charles B., Jr. (1970), *College Calculus with Analytic Geometry* (2nd ed.), Reading: Addison-Wesley, LCCN 76087042.

Ray W. Clough. (1960). *The Finite Element Method in Plane Stress Analysis*. American Society of Civil Engineers.

Silva, V. D. d., (2006). The Strain Tensor. In: *Mechanics and Strength of Materials*. Springer, p41-64.

Silva, V. D. d., (2006). The Stress Tensor. In: *Mechanics and Strength of Materials*. s.l.:Springer, pp. 9-37.

Tabatabaian, M. (2015). *COMSOL5 for Engineers*. Bloomfield: Mercury Learning & Information.

Urugal, A.C & Saul K. Fenster. (1975). *Advanced strength and applied elasticity.* American Elsevier.

Walter and Deborah, (2008). Definition and Design Relations. In: Peterson's *Stress Concentration Factors*, Third Edition. s.l.:John Wiley & Sons, Inc., pp. 1-54.

8. APPENDIX

Table 1. Results of FEA testing and calculations for deflection which shows the differences between solid and beam elements by length-to-span ration. (GoEngineer 2016, accessed on 27 Feb. 2020)

		Deflection			
Beam Length (mm)	Analytical (mm)	Beam (mm)	% error	Solid (mm)	% error
15	0.0011	0.0014	20.51%	0.0006	-94.09%
20	0.0026	0.0030	12.69%	0.0030	15.13%
30	0.0087	0.0093	6.07%	0.0094	6.89%
40	0.0207	0.0215	3.52%	0.0215	3.65%
50	0.0404	0.0414	2.27%	0.0413	2.18%
60	0.0698	0.0710	1.58%	0.0708	1.36%
70	0.1109	0.1122	1.15%	0.1119	0.88%
80	0.1656	0.1671	0.92%	0.1666	0.62%
90	0.2357	0.2374	0.70%	0.2367	0.41%
100	0.3234	0.3252	0.57%	0.3242	0.26%
120	0.5588	0.5610	0.40%	0.5594	0.11%
140	0.8873	0.8899	0.29%	0.8875	0.02%
160	1.3245	1.3280	0.26%	1.3240	-0.04%
180	1.8858	1.8890	0.17%	1.8850	-0.05%
200	2.5869	2.5910	0.16%	2.5850	-0.07%

Table 2. Results of FEA testing and calculations for stress which shows the differences between solid and beam elements by length-to-span ration. (GoEngineer 2016, accessed on 27 Feb. 2020)

		Stress			
Beam Length (mm)	Analytical (MPa)	Beam (MPa)	% error	Solid (MPa)	% error
15	15.28	15.28	0.01%	11.71	-30.48%
20	20.37	20.37	-0.01%	18.98	-7.33%
30	30.56	30.56	0.01%	28.54	-7.07%
40	40.74	40.74	-0.01%	40.36	-0.95%
50	50.93	50.93	0.00%	50.12	-1.62%
60	61.12	61.12	0.01%	59.83	-2.15%
70	71.30	71.3	0.00%	67	-6.42%
80	81.49	81.49	0.00%	76.45	-6.59%
90	91.67	91.67	0.00%	90.17	-1.67%
100	101.86	101.9	0.04%	100.3	-1.55%
120	122.23	122.2	-0.03%	116.4	-5.01%
140	142.60	142.6	0.00%	140.7	-1.35%
160	162.97	163	0.02%	156.9	-3.87%
180	183.35	183.3	-0.03%	180.9	-1.35%
200	203.72	203.7	-0.01%	197.4	-3.20%

Table 3: *Mechanical property of aluminium (Comsol Material Library).*

Density	rho	2700[k...	kg/m³
Young's modulus	E	70e9[Pa]	Pa
Poisson's ratio	nu	0.33	1
Relative permeability	mur_i...	1	1
Heat capacity at constant p...	Cp	900[J/(...	J/(kg·...

Table 4. The maximum shear stress and twist angle of a square cross section. (Hibbeler 2018 p.248)

Shape of cross section	τ_{max}	ϕ
Square a × a	$\dfrac{4.81\,T}{a^3}$	$\dfrac{7.10\,TL}{a^4 G}$

Table 5. Constant of torsion Equations (3-7) and (3-8) (Urugal, A.C & Saul K. Fenster 1975).

b/t	1.00	1.50	1.75	2.00	2.50	3.00	4	6	8	10	∞
α	0.208	0.231	0.239	0.246	0.258	0.267	0.282	0.299	0.307	0.313	0.333
β	0.141	0.196	0.214	0.229	0.249	0.263	0.281	0.299	0.307	0.313	0.333

Table 6. The angle of twist of I-section beam due to torsion (engineer-inglibrary.org. (n.d.). Beam Torsion | Engineering Library, accessed 27 Feb. 2020).

Table 7. Mathematical results of surface load situation.

Surface load	Maximum normal stress (MPa)	Maximum displacement (mm)
Rectangular beam (0,08 m*0,03 m)	75	6,45
Square beam (0,08 m*0,08 m)	10,55	0,339
I-beam (0,03 m thick)	77,14	6,61
I-beam (0,08 m thick)	15,4	0,495

Table 8. Mathematical results of axial load situation.

Axial load	Maximum normal stress (MPa)	Maximum displacement (mm)
Rectangular beam (0,08 m*0,03 m)	0,42	3,57E-03
Square beam (0,08 m*0,08 m)	0,16	1,34E-03
I-beam (0,03 m thick)	0,56	4,78E-03
I-beam (0,08 m thick)	0,36	3,06E-03

Table 9. Mathematical results of torsion situation.

Torsion	Maximum normal stress (MPa)	Twist angle (rad)
Rectangular beam (0,08 m*0,03 m)	26,7	0,021
Square beam (0,08 m*0,08 m)	4,7	1,98E-03
I-beam (0,03 m thick)	77,14	0,661
I-beam (0,08 m thick)	15,4	4,27E-03

Figure 10. Comparison between Euler-Bernoulli and Timoshenko theory. (accessed at 10/12/2019)
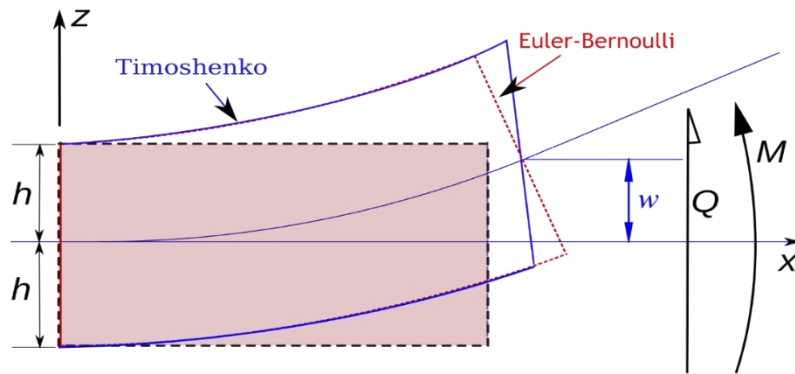

Figure 24. Formulation of Euler-Bernoulli is used for analysis, gao jie, 19/03/2020.
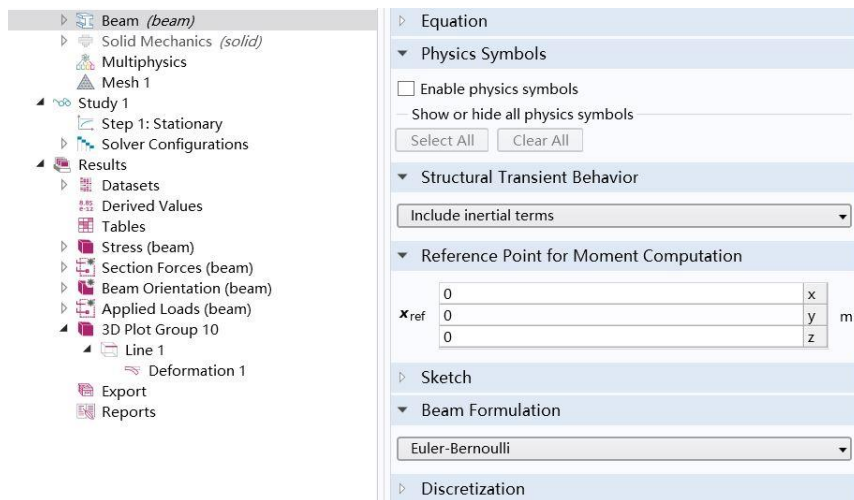
Table 10. Results of surface load occasion.

Surface load	Rectangular (0,08m*0,03m)	Square (0,08m*0,08m)	I-beam (0,03m thick)	I-beam (0,08m thick)
Mathematical calculation				
Maximum normal stress (MPa)	75	10,55	77,14	15,4
Maximum displacement (mm)	6,45	0,339	6,61	0,495
Solid mechanics				
Maximum normal stress (MPa)	79	13,7	79,6	20,8
Maximum displacement (mm)	5,75	0,308	6,64	0,521
Euler-Bernoulli formulation				
Maximum normal stress (MPa)	75	10,5	77,1	15,4
Maximum displacement (mm)	6,45	0,339	6,61	0,496
Timoshenko formulation				
Maximum normal stress (MPa)	75	10,5	77,1	15,4
Maximum displacement (mm)	6,45	0,345	6,61	0,517

Table 11. Results of axial load occasion.

Axial load	Rectangular (0,08m*0,03m)	Square (0,08m*0,08m)	I-beam (0,03m thick)	I-beam (0,08m thick)
Mathematical calculation				
Maximum normal stress (MPa)	0,42	0,16	0,56	0,36
Maximum displacement (mm)	3,57E-03	1,34E-03	4,78E-03	3,06E-03
Solid mechanics				
Maximum normal stress (MPa)	0,527	0,221	0,744	0,532
Maximum displacement (mm)	3,56E-03	1,33E-03	4,75E-03	3,05E-03
Euler-Bernoulli formulation				
Maximum normal stress (MPa)	0,42	0,16	0,56	0,36
Maximum displacement (mm)	3,57E-03	1,34E-03	4,76E-03	3,06E-03
Timoshenko formulation				
Maximum normal stress (MPa)	0,42	0,16	0,56	0,36
Maximum displacement (mm)	3,57E-03	1,34E-03	4,76E-03	3,06E-03

Table 12. Results of torsion occasion.

Torsion	Rectangular (0,08m*0,03m)	Square (0,08m*0,08m)	I-beam (0,03m thick)	I-beam (0,08m thick)
Mathematical calculation				
Maximum normal stress (MPa)	26,7	4,7	72,14	15,4
Twist angle (rad)	0,021	1,98E-03	0,661	3,07E-03
Solid mechanics				
Maximum normal stress (MPa)	29,4	5,41	74,4	16,9
Twist angle (rad)	2,80E-02	2,03E-03	4,75E-03	3,15E-03
Euler-Bernoulli formulation				
Maximum normal stress (MPa)	26,6	4,7	72,1	15,4
Twist angle (rad)	0,021	1,98E-03	0,661	3,08E-03
Timoshenko formulation				
Maximum normal stress (MPa)	26,7	4,7	72,1	15,4
Twist angle (rad)	0,021	1,99E-03	0,662	3,11E-03